4. MIDDLE-1823 STRATIGRAPHY AND GEOHYDROLOGY BASED ON LITHOLOGICAL AND GEOPHYSICAL LOGS

Areas of study addressed in this section include the vadose zone, the aquifer, and the subaquifer zone, as follows:

The Vadose Zone. The rocks of Well Middle-1823 are mostly basalt with occasional poorly consolidated sedimentary interbeds above ~4,042 ft MSL (~900 ft bls). The temperature minimum at ~4,657 ft MSL (~285 ft bls) is strongly suggestive of an inflow of cold material into the borehole, which in the winter could be either a perched water layer, infiltrating snow-melt water, or, more likely, the flow of air through fractured basalt—a very common phenomenon on the ESRP. Since the neutron log indicates that this interval is H poor, and since the temperature on February 19, 2003, was below freezing for most of the day[c] (Hukari 2003[d]), the flow of air is more probable than the flow of water through the vadose zone.

An interval of interbedded sediments and basalts occurs in the vadose zone from ~4,772 to ~4,622 ft MSL (~170 to ~320 ft bls). Within this interval, the lithological and neutron logs indicate that a silty sand and gravel bed at ~4,722 ft MSL (~220 ft bls) might be water-saturated. The temperature there is near a local maximum but the temperature gradient is negative, suggesting that there was not a large amount of water flowing through this interbed on the day that the temperature log was collected. At ~4,677 ft MSL (265 ft bls), the neutron flux reaches a maximum for the borehole, indicating very dry conditions. Based on the neutron and NGR logs, the rocks from this depth to the top of the aquifer are a sequence of relatively dry basalts, excluding an interbed at ~4,642 ft MSL (~300 ft bls). At ~4,465 ft MSL (~477 ft bls), there is an extremely sharp rise in temperature and a strongly positive temperature gradient, suggesting an interval through which there is no flow of either air or water. This interval is immediately above the top of the aquifer.

The Aquifer. The neutron and temperature logs show that the top of the aquifer is at 4,452 ft MSL (~490 ft bls) and the bottom is at ~3,912 ft MSL (~1,030 ft bls). From just above the top of the aquifer to below ~4,342 ft MSL (~600 ft bls) there are several sequences of rubble and thinly bedded, scoriaceous, near-vent basalts. The slope of the temperature log is slightly less steep in this interval, possibly reflecting slightly lower transmissivity in these near-vent facies as compared to less disturbed basalts below ~4,242 ft MSL (~700 ft bls) where conditions are isothermal. At ~4,000 ft MSL (~942 ft bls), there is a small positive temperature inflection and an increased gradient, probably due to the choking off of permeability by the growth of alteration minerals (Morse and McCurry 2000). Flow is completely choked off below the base of the aquifer at ~3,912 ft MSL (~1,030 ft bls).

The Subaquifer Zone. Below ~3,912 ft MSL (~1,030 ft bls), the temperature increases along the ambient lithostatic gradient. Below ~3,842 ft MSL (~1,100 ft bls), basalts become increasingly altered. More than half of the rocks exposed in the subaquifer are sedimentary interbeds with three 40-ft-thick clayey silty sand layers between ~3,862 to ~3,682 ft MSL (~1,080 and ~1,260 ft bls) and a 250-ft layer of interbedded sands, silts, and clays below ~3,653 ft MSL (~1,290 ft bls). Due to the anomalous behavior of the neutron log in the subaquifer zone, it is difficult to determine if there are any confined or semiconfined aquifers in this interval. The temperature gradient is positive throughout the subaquifer zone even in the thick sediments, which argues against any confined aquifers, with one possible exception. At ~3,785 ft MSL (~1,157 ft bls), it is possible that a thin, confined aquifer is present since the temperature gradient at this depth is negative.

---

c. For the period of 8 a.m. to 5 p.m. on February 5, 2003, at TRA, temperatures were: low = +22°F, high = +33.2°F, and an average = +26.8°F. Wind velocities were: low = 0.6 mph, high = 8.5 mph, and an average = 3.5 mph.

d. Hukari, N., National Oceanic and Atmospheric Association, personal communication to C. Helm-Clark, INL, September 2003.

4.1 Methods of Stratigraphic Correlation

The focus of this study was the stratigraphy of Borehole Middle-1823 and its relationship to the stratigraphy of other nearby boreholes. In general, this study used the interpretive guidelines for logging in basalt from Helm-Clark, Rodgers, and Smith (2004). For the purposes of comparison, a detailed stratigraphic column was made for every borehole and/or well in the study area based on lithological and geophysical logs. (See Figure A-1 [Appendix A] for detailed stratigraphy for Middle-1823.) After individual stratigraphic columns were constructed, these were compared to columns for neighboring wells, in addition to all available geochronological, paleomagnetic, and geochemical information. On the basis of the comparisons, shared stratigraphy was correlated wherever possible.

4.1.1 Data Collection

Data were gathered for all wells in the environs of TRA and for wells that penetrated the aquifer elsewhere. Some wells were included in the study because geochronological data were available (e.g., USGS-121). Other wells were included because geochemical data were available. Four wells (i.e., C1A, INEL-1, WO-2 and Corehole 2-2A) were included in the study because of their depth and the presence of deep sediments (>1,000 ft bls).

The role of careful data gathering cannot be overemphasized. For example, a thorough mining of the Hydrogeological Data Repository files revealed three different lithological logs for INEL-1, all of which were different, and two of which had been published. It is unfortunate, but true, that there could be two or more contradictory lithological logs for a borehole or well. Due to this circumstance, it is important to find all the logs for a borehole and then use the wireline logs to identify the better lithological log where two or more were available.

4.1.2 Depth Control

Lithology logs were adjusted using standard half-height depth picks from the NGR log. Overall, depth adjustment of the data was complicated by the fact that depth control for INL wells is generally uncertain. Few wireline logs indicate what type of depth control was used (referenced to ground surface, casing lip, bench mark, etc.). In addition, the tops of many older wells were reworked in the 1992–1994 period to upgrade them to Idaho well construction standards. There is often no notation in the well maintenance records as to whether a bench mark was added or moved, or if ground surface referencing was changed because of the addition of a well pad. Poor depth control complicates the effort to adjust depths between older and younger wireline logs. The standard method for depth adjustment (i.e., comparing NGR logs) is not always possible since an NGR log is not collected on every logging run. It is not uncommon to see depth discrepancies of 5 ft or more between logs.

Based on observations on two occasions during 2003, it was noted that the United States Geological Survey (USGS) logging crew visually estimated the alignment of the wireline tools inside the casing with the surface of the ground without measuring with a level and tape. There are few records, however, documenting how the USGS establishes the zero depth measuring point for their wireline sondes. The depth discrepancy problem also occurs in well documentation because the elevation measuring point is seldom recorded. The problem is more widespread than just in the USGS records, and it extends to both new and old geologists' and drillers' logs. It is also not a new problem since it was mentioned as early as Jones, Jones, and Crosthwaite (1953) and discussed in detail in Chase et al. (1964) and other Site reports. Because of the history of poor depth control for INL wells, this study assumes that depths can be up to 5 ft in error. When constructing stratigraphic columns, unit depths were often rounded to the nearest 5 ft, especially when wireline logs were noisy or the quality of lithological logs was poor.

4.1.3 Data Interpretation

Each stratigraphic column shown on the fence diagrams and cross sections (Appendix A) is an interpretation of all the information available. In general, the descriptions of units on the stratigraphic columns are exact quotes or close paraphrasing from the lithological logs. In many places, a unit will have a description similar to "minor NGR peak." These are from boreholes where there is a distinct feature on one or more of the wireline logs but no information on the lithological log. When a peak or trough is not labeled, it is safe to assume that the feature in question occurs on a natural gamma log. For wells and boreholes with available geochronology data, both paleomagnetic inclination in degrees and age dates in ka are listed on the stratigraphic columns. Where water level information and USGS I-Flow picks are available, these also are included in the stratigraphic columns.

Some of the units shown on the stratigraphic columns are composite features. Some are based on NGR, N, and DEN shape matching where the shape is distinctive and recognizable in more than one borehole, and where the variation of amplitude for the shape indicates that more than one rock type is present. Other composite units occur because that is how they were originally logged on a driller's or geologist's log. Some logged basalt units can be a composite of more than one flow group; these can be difficult to identify if there is low contrast between flow groups on the geophysical logs. All three composite unit types occur on the fence diagrams and cross sections.

Since units that are far apart can have very similar age dates and paleomagnetic inclinations, any correlations between such units rely on geochemical analyses wherever possible. The addition of geochemistry data is often diagnostic where it is available. Fortuitously, geochemical data exists for most INL boreholes that have been sampled for paleomagnetic studies. Where geochronological information is absent, most of the stratigraphic correlations rely heavily on the stratigraphic columns synthesized for each well or borehole. Shape matching of wireline data is the least preferred method of correlation (except where no other data are available). Shape matching is used, however, to check and confirm correlations already made.

Geochronological data and geochemical data for the central areas of INL are summarized in Tables 4-1 and 4-2. The geochronology data are obtained from several sources. Age dates determined through volcanic recurrence analysis are not used. As much as possible, pooled or averaged age dates also are not used. Pooled and recurrence analysis ages are calculated on the basis of already-determined stratigraphic correlations. For the purposes of establishing a new site stratigraphy, it is not appropriate to use dates based on a previous stratigraphic interpretation. All paleomagnetic inclination data was obtained from Duane Champion at the USGS, some of which have not been published. The geochemistry data is from the Idaho State University (ISU) ESRP geochemistry database maintained by Scott Hughes and Michael McCurry at the ISU Geology Department. The database used for this study is an expanded version of that published in Geological Society of America Special Paper 353 (Hughes, McCurry, and Geist 2002), provided by Prof. Hughes in December 2002.

Most of the fence diagrams and cross sections concentrate on the TRA well field, although three of these include a limited number of wells and boreholes at INTEC and NRF. The fence diagrams were made to establish a detailed stratigraphy of the TRA well field and to place Middle-1823 within that stratigraphy. The cross sections were made to study and correlate the deep sediments in Middle-1823 with other wells and to explore issues related to structure and geochronology.

Table 4-1. Test Reactor Area age dates and paleomagnetic inclination data.

Unit	Max Elev. (ft)	Min Elev. (ft)	Est. Avg. Thickness	Inclination	Location	Reference*	Age Date	Dating Method	Location	Reference*
TRA-B1	4,880	4,840	15	54.5°±1.3°	USGS-80	OFR 93-327	419±33 ka	K/Ar	USGS-80	OFR 93-327
TRA-I1	4,860	4,840	6							
TRA-B2	4,860	4,825	16	67.0°±2.9°	TRA-5A/PZ1	DC Aug 2002				
TRA-I2	4,865	4,760	10							
TRA-B3	4,840	4,755	37	76.6°±1.2°	TRA-5A/PZ1	DC Aug 2002	461±24 ka	K/Ar	USGS-80	OFR 93-327
				74.9°±3.5°	USGS-80	DC Aug 2002	414±8 ka	Pooled date	USGS-80, TRA-5A/PZ1	Champion et al. (2002)
				72.8°±2.2°	ICPP-SCI-V-213	DC May 2003				
				77.4°±1.2°	ICPP-SCI-V-214	DC May 2003				
TRA-I3	4,805	4,730	13							
TRA-B4	4,790	4,735	17	58.4°±3.6°	TRA-5A/PZ1	DC Aug 2002				
				59.6°±4.8	USGS-80	OFR 93-327				
TRA-I4	4,770	4,720	28							
TRA-B5	4,760	4,715	20	74.0°±2.4°	TRA-5A/PZ1	DC Aug 2002				
				71.1°±1.4°	ICPP-SCI-V-214	DC May 2003				
				72.2°±0.9°	ICPP-SCI-V-213	DC May 2003				
TRA-I5	4,730	4,705	14							
TRA-B6	4,740	4,650	16	56.7°±0.9°	TRA-5A/PZ1	DC Aug 2002	643±64 ka	K/Ar	USGS-80	OFR 93-327
				53.9°±1.9°	USGS-80	OFR 93-327	626±67 ka	K/Ar	AEC Butte	Champion et al. (1988)
				53.5°±1.6°	AEC Butte	Champion, Lanphere, and Kuntz (1988)	637±35 ka	Pooled date	USGS-80, USGS-123, AEC Butte	Champion et al. (2002)
TRA-I6	4,650	4,640	10							
TRA-B7	4,650	4,620	23	53.4°±1.5°	TRA-5A/PZ1	DC Aug 2002	786±23 ka	K/Ar	TRA-5A/PZ1	Champion et al. (2002)
TRA-I7	4,650	4,620	20							
TRA-B8	4,620	4,570	30							

* **NOTE:** OFR 93-327 = Lanphere, Champion, and Kuntz (1993). DC = Champion, D., USGS, personal communications to S. Ansley; the date of these communications is given in the table. These paleomagnetic data are preliminary results, may be subject to change, and have not been peer-reviewed. These data are included here merely as indicators of what the final paleomagnetic inclination results may look like once published. They were provided as a courtesy and should not be quoted without consulting Dr. Champion.

Table 4-2. Age dates and paleomagnetic inclination data for the Idaho Nuclear Technology Engineering Center, New Production Reactor, and Naval Reactors Facility.

a. New Production Reactor site age date and paleomagnetic data.

NPR-Test/WO-2*	Flow Groupings from Previous Studies for NPR-Test/WO-2*							Corresponding Flow Groups from this Study for NPR-Test/WO-2*	
Inclination or Chron of Flow	Top Elev. of Flow (ft)	Bottom Elev. of Flow (ft)	Age Date	Dating Method	Borehole or Well	Rock Type	Reference**	Top Elev. of Flow (ft)	Bottom Elev. of Flow (ft)
54.9°±0.8°	4,923	4,827	233±34 ka	K/Ar	NPR-Test	basalt	DC88, DC02	4,903	4,831
63.6°±0.9°	4,818	4,797			NPR-Test	basalt	DC88, DC02	4,823	4,790
72.8°±1.0°	4,794	4,687	350±40 ka	K/Ar	NPR-Test	basalt	DC88, DC02	4,776	4,689
63.0°±1.2°	4,663	4,633			NPR-Test	basalt	DC88, DC02	4,666	4,632
56.3°±0.6°	4,627	4,531	441±77 ka	K/Ar	NPR-Test	basalt	DC88, DC02	4,625	4,540
60.1°±1.8°	4,506	4,474	491±80 ka	K/Ar	NPR-Test	basalt	DC88, DC02	4,525	4,480
-40.8°±2.7°	4,474	4,439			NPR-Test	basalt	DC88, DC02	4,474	4,442
66.4°±1.4°	4,438	4,373	580±93 ka	K/Ar	NPR-Test	basalt	DC88, DC02	4,438	4,375
52.9°±1.6°	4,334	4,236	641±54 ka	K/Ar	NPR-Test	basalt	DC88, DC02	4,327	4,233
Bruhnes Chron	4,236	4,220	<780 ka	Paleomagnetic	WO-2	basalt	DC02	4,229	4,218
***	4,220	4,162			WO-2	sediments	DC02	4,216	4,157
Matuyama Chron (negative polarity)	4,162		>780 ka	Paleomagnetic	WO-2	basalt	DC02	4,157	
	3,679	3,630	982±53 ka	$^{40}Ar/^{39}Ar$	WO-2	basalt	A97	3,679	3,630
Olduvai Subchron	3,233	3,196	1.086±0.24 Ma	$^{40}Ar/^{39}Ar$	WO-2	basalt	A97	3,233	3,196

* NPR-Test and WO-2 are located next to each other. Since NPR-Test was logged and cored to 602 ft bls and WO-2 was logged and cored below ~600 ft bls, the logs for these two wells are usually combined and presented as a composite labeled as NPR-Test/WO-2 or, more often, as just WO-2. Most WO-2 logs with information between 0 and 600 ft bls are composite logs.

** Reference Key:
A97 = Anderson, Liszewski, and Cecil (1997)
DC88 = Champion, Lanphere, and Kuntz (1988)
DC02 = Champion et al. (2002).

*** It is not clear in Champion et al. (2002) whether the sediment layer at the Bruhnes-Matuyama boundary belongs to the Matuyama or is undated.

Table 4-2. (continued).
b. INTEC/USGS-121 age date and paleomagnetic data.

USGS-121 Flow No. from DC02	Flow Groupings Sampled for Ages and Inclinations from DC02		Paleomag Inclination in Degrees from J&C96	Age Date in ka ("kilo-anno")	Dating Method	Age Date Reference	Corresponding Flow Groups for this Study	
	Top Elev. of Flow (ft)	Bottom Elev. of Flow (ft)					Top Elev. of Flow (ft)	Bottom Elev. of Flow (ft)
1	4,876	4,857	56.8°±2.3°	77±39 ka	K/Ar or $^{40}Ar/^{39}Ar$	DC02	4,880	4,853
2	4,857	4,818	61.5°±2.1°				4,853	4,826
3	4,818	4,796	75.6°±2.5°				4,814	4,798
4	4,796	4,780	53.0°±2.0°					
5	4,776	4,722	54.0°±2.6°	376±81 ka	K/Ar or $^{40}Ar/^{39}Ar$	DC02	4,781	4,774
							4,767	4,728
6	4,722	4,666	54.6°±1.4°				4,728	4,706
							4,706	4,667
7	4,662	4,586	53.3°±2.3°				4,665	4,587
8	4,586	4,518	53.5°±1.7°	543±48 ka	K/Ar or $^{40}Ar/^{39}Ar$	DC02	4,582	4,514
9	4,498	4,492	61.5°±7.6°				4,503	4,492
10	4,488	4,442	66.1°±2.3°	616±61 ka	K/Ar or $^{40}Ar/^{39}Ar$	DC02	4,483	4,442
11	4,442	4,388	68.0°±1.2°				4,436	4,391
12	4,385	4,370					4,386	4,376
13	4,370	4,324	57.6°±0.9°				4,376	4,368
							4,368	4,330
14	4,324	4,308	50.9°±2.1°				4,322	4,267
15	4,307	4,266	58.3°±0.8°					
16	4,266	4,206	65.6°±1.5°				4,262	4,233
							4,228	4,204
17	4,206	4,176	57.6°±2.4°	759±12 ka	K/Ar or $^{40}Ar/^{39}Ar$	DC02	4,204	EOL 4193

EOL = End of Log Data.

Reference Key:
J&C96 = Jobe, S., and D. Champion, USGS, unpublished data, 1996
DC02 = Champion et al. (2002).

NOTE: USGS-121 is a deviated well where there may be some question as to the quality of the deviation log (Rohe 2004[e]). Below 540 ft bls, the borehole bridged before deviation data could be collected. The deviation is thought to be greater than 1° to 3° too steep: the correction to remove the vertical tilt from these data is unknown and therefore was never applied to the data reported. Most of the differences between the depths reported in Champion et al. (2002) and the ones determined for this study are likely due to differences in reported interbed thicknesses. In general, collected cores tend to lose some material when sampling is attempted in unconsolidated sediments, so core logs can underestimate bed thicknesses; whereas geophysical logs may see intertrappean material both above and below actual interbed depths due to "seeing" any sediments that have infiltrated basalt fractures in the flow tops and bottoms that sandwich interbeds. Any depth picks for USGS-121 should be considered to have much more error than for most of the boreholes on-Site, since few share the problems it has with deviation.

e. Rohe, M., 2004, personal communication to C. Helm-Clark, March 2004.

Table 4-2. (continued).
c. INTEC/USGS-123 age date and paleomagnetic data.

USGS-123 Flow No. from L93*	Flow Groupings Sampled for Ages and Inclinations		Paleomag Inclination in Degrees	Age Date in ka ("kilo-anno")	Dating Method	Corresponding Flow Groups for this Study	
	Top Elev. of Flow (ft)	Bottom Elev. of Flow (ft)				Top Elev. of Flow (ft)	Bottom Elev. of Flow (ft)
1	4,887	4,813	53.4°±1.3°	219±50 ka	K/Ar	4,890	4,816
2	4,806.5	4,802	56.5°±12.9°			4,805	4,803
3	4,801	4,765	54.2°±2.8°			4,802	4,789
						4,789	4,767
4	4,756	4,713	72.7°±1.1°			4,760	4,716
5	4,710	4,671	61.7°±1.7°			4,712	4,672
6	4,671	4,640	58.3°±2.4°			4,672	4,644
7	4,635	4,537	57.2°±2.1°	466±39 ka	K/Ar	4,636	4,617
						4,617	4,538
8	4,537	4,499	60.6°±1.4°			4,534	4,500
9	4,495.5	4,422.5	65.9°±1.8°			4,496	4,479
						4,477	4,421
10	4,422.5	4,410	60.9°±7.3°			4,421	4,418
						4,416	4,411
11	4,410	4,355.5	68.7°±1.8°	619±22 ka	K/Ar	4,411	4,360
12**	4,355.5	4,232	54.8°±2.6°	737±29 ka**	K/Ar**	4,356	4,233
13	4,228	4,194.5	56.4°±2.7°	653±49 ka	K/Ar	4,229	4,196
14	4,194.5	4,178.5	57.6°±3.3°			4,196	4,180

* All age and inclination data from Lanphere, Champion, and Kuntz (1993) ("L93").
** An unsuccessful age date measurement was attempted by Lanphere, Champion, and Kuntz (1993) for this flow.

NOTE: USGS depths are often corrected for deviation, while the depths taken from the raw data analyzed for this study are uncorrected. Most well deviation errors at INL are smaller than the USGS estimated error of 2 ft for their depth picks (Anderson et al. 1996). The deviation for USGS-123, calculated from magnetic deviation sonde data, shows less than 0.1 ft of deviation at the water table. Most of the differences in flow depths between data from Lanphere, Champion, and Kuntz (1993) and this study are less than the estimated error reported by the USGS. In most other cases, the difference is the result of how the thickness of interbeds and other intertrappean materials are recorded: in general, collected cores tend to lose some of the unconsolidated sediments, so core logs can underestimate these thicknesses; whereas geophysical logs tend to see interbeds both above and below actual interbed depths due to "seeing" infiltrated sediments in the fractures in the basalt flow tops and bottoms that sandwich sedimentary beds.

Table 4-2. (continued).
d. Naval Reactors Facility area age date and palemogagnetic data.

NRF Flow Order on Cross Section O - O'	Paleomagnetic Measurements					Radiometric and Paleomagnetic Age Date Measurements					
	Sample Location	Top Elev. of Flow Sampled	Bottom Elev. of Flow Sampled	Inclination of Flow	Ref.*	Sample Location	Top Elev. of Flow Sampled	Bottom Elev. of Flow Sampled	Age Date	Dating Method	Ref.*
1	NRF-89-05	4,829	4,743	73.3°±1.5°	L93	NRF-89-05	4,829	4,743	303±30 ka	K/Ar	L93
2	NRF-89-05	4,732	4,656	55.6°±0.7°	L93	NRF-6P	4,758	4,682	395±25 ka	K/Ar	DC02
3	NRF-89-05	4,654	4,642	61.5°±17.0°	L93	NRF-89-05	4,654	4,642	492±56 ka	K/Ar	L93
4	NRF-89-05	4,642	TD 4,608	66.5°±3.0°	L93	NRF-89-04/05	**	**	521±21 ka	K/Ar	DC02
	NRF-89-04	4,653	4,631	66.1°±3.0°	L93	NRF-89-05	4,642	TD 4,608	533±37 ka	K/Ar	L93
5	NRF-89-04	4,628	TD 4,601	71.2°±2.1°	L93	NRF-6P	4,637	4,494	546±47 ka	$^{40}Ar/^{39}Ar$	DC02
6						NRF-6P	4,493	4,429	727±31 ka	$^{40}Ar/^{39}Ar$	DC02
7	NRF-7	4,439	4,418	Normal	DC02	NRF-7	4,439	4,418	<780 ka	Paleomag	DC02
8	NRF-7	4,415	TD 4,342	Reversed	DC02	NRF-7	4,415	TD 4,342	884±53 ka	$^{40}Ar/^{39}Ar$	DC02

NOTE: Flow tops and bottoms here (and on Cross Section O-O', Figure A-16, Appendix A) are from Champion et al. (2002).

* L93 = Lanphere, Champion, and Kuntz (1993); DC02 = Champion et al. (2002).
** Champion et al. (2002) listed the date as being for flow 4 in both borehole NRF-89-04 and borehole NRF-89-05.

TD = "Total Depth" elevations with TD annotation denote the bottom of the well and not necessarily the bottom of NRF flow 8.

Historically, especially on older logs, the term “cinders” has been used as a catch-all term for various intertrappean materials including sediments, infiltrated loess, actual cinders and ash, basalt rubble, igneous rocks with perlitic textures, scoria, glassy rims at the top of flows, and other volcanic glasses (Chase et al. 1964). A cinder layer, therefore, is not always a cinder *sensu stricto* on the stratigraphic columns.

The correlations shown on the cross sections and fence diagrams (Appendix A) are relatively conservative. No correlations were forced for the sake of constructing a complete surface-to-subaquifer stratigraphy appropriate for groundwater modeling. Most of the correlations are based on at least three lines of evidence (lithology logs, NGR logs, and some combination of DEN, N, caliper, and/or temperature logs). Many correlations are not of formation units but of features like a distinctive pattern of NGR or DEN peaks, a set of distinctive elemental concentrations at a certain depth, a contact between a basalt and an interbed, or a pattern of paleomagnetic inclination data.

In time, as more data gaps are filled, it is likely that some of the correlations from this study will require revision, especially for wells and boreholes where no geophysical logs have ever been collected or where only an NGR log exists with no accompanying lithology information.

4.2 Stratigraphic Analysis of the Test Reactor Area Well Field

To place Middle-1823 within the context of the Site stratigraphy, we must first ascertain the nature of the local stratigraphic framework. To do that, we start with wells that provide some geochronological control. The geochronology data for the TRA well field discussed in this section is summarized in Table 4-1.

The two wells in the TRA environs both with paleomagnetic inclination and radiometric age data are USGS-80 and TRA-5A.[f] Correlating units between these two locations should establish a useable geochronology for most of the TRA well field. Since the stratigraphy of USGS-80 incorporates Qbd-age basalts at shallow levels, it is advisable to consider all other shallow wells, as well as aquifer wells. Figure 4-1 shows a map of the TRA well field and environs.

Fence diagram A-A' (Figure A-2) shows a traverse from USGS-80 to TRA-6A. Units that are correlated in two or more wells with confidence are shaded in color. Well USGS-80 provides age and/or inclination data for four basalt units. All of the uppermost TRA basalt units occur at this location, named here as TRA-B1 through -B4 for convenience in this study. Basalt TRA-B2 (light blue on fence diagram A-A') has been segregated from the TRA-B3 (light green) basalt below for two reasons: (1) there are at least two, and possibly three basalt units above TRA-B3, based on stratigraphy data closer to TRA; and (2) there is a paleomagnetic inclination data point very close in value to inclinations of the uppermost basalt in TRA-5A. The number of basalt units above TRA-B3 varies from one to two (and rarely three) as they pinch in and out between USGS-80 and the TRA fence line. In general, TRA-B2 thickens to the west.

f. There are two wells in the TRA well field with very similar names: TRA-5 and TRA-5A. TRA-5 is the TRA disposal well, with a fair-to-good lithological log and several geophysical logs. TRA-5A is sometimes denoted as TRA-5A/PZ1. This ~300-ft deep borehole was cored from the surface but had to be abandoned before a well could be built. As a result, cores from this borehole have been analyzed for geochemical and paleomagnetic studies, but no detailed lithological log was made from those cores, and no geophysical logs were collected for this location.

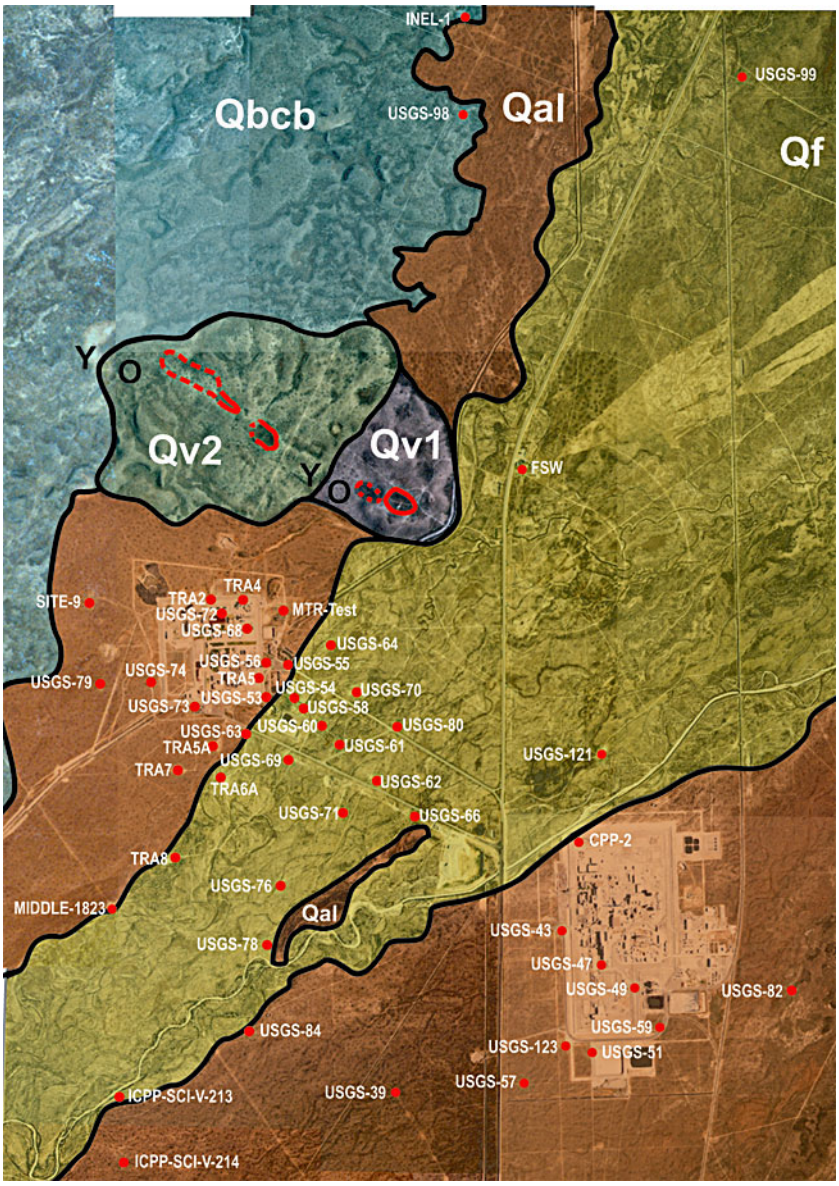

NOTE: *The wells shown are those analyzed for this project. Well WO-2, east of INTEC, and the wells at the NRF are outside the area of this figure. The TRA well field includes all the wells south of AEC Butte (labeled Qv1) and the Qv2 fissure vent and west of Lincoln Boulevard. Wells USGS-39, USGS-84, ICPP-SCI-V-213, and ICPP-SCI-V-214 are closer to CFA than TRA, but for the purposes of this report, they are included as the extreme southern edge of the TRA well field.*

Figure 4-1. Map of the Test Reactor Area well field and environs.

Basalt TRA-B1 has an age date of 419 ka. TRA-B3 has a date of 461 ka, but it also has a published pooled date of 414 ka (Champion et al. 2002). We have given the 461 ka date precedence over the pooled date for the reasons given in the methodology section above. The bottom basalt in USGS-80 is TRA-B6, dated at 643 ± 64 ka, which we can correlate to the basalt of the AEC Butte at 626 ka. Basalts TRA-B4 and TRA-B6 both deepen and thicken to the southwest. Basalt TRA-B5 (brown) is present in USGS-65 and TRA-6A but pinches out northward before it can reach USGS-63 and Monroe Boulevard.

Fence diagram B-B' (Figure A-3) shows the short traverse from USGS-80 to USGS-71. Unit TRA-I1, the intertrappean layer between TRA-B1 and TRA-B2, and basalt TRA-B2 both thicken and deepen to the southwest. This is a common pattern in this part of the TRA well field. In USGS-62, TRA-B3 (light green) resembles thinly bedded and disturbed basalt, more evocative of near-vent facies than the more coherent basalts in the equivalent stratigraphic positions in USGS-80 and USGS-71. Fence diagram C-C' (Figure A-4) shows a traverse from USGS-70 to USGS-71, which is closer to TRA-5A where we want to end up. The pattern of deepening and thickening in TRA-B2 is apparent. TRA-B3 also deepens to the south, though most of these wells do not penetrate the base of this basalt, so we cannot be sure it also thickens.

Fence diagram D-D' (Figure A-5) shows a northwest-southeast traverse from USGS-66 to USGS-58. In general, these correlated units are mostly flat in the upper 400 ft, which is what one would expect in an area where deepening is in a southwesterly direction away from the vents Qv1 (AEC Butte) and Qv2; strata perpendicular to the direction of steepening is approximately level, barring minor local undulations of flow surfaces typical of most ESRP basalts. Well USGS-58 shows basalts TRA-B7 (dark pink) and TRA-8 (light violet). TRA-B8 is not the same as the composite sediment/cinder/rubble unit (light violet with stripes) under TRA-B7 in USGS-66. Well USGS-66 is a very interesting location geologically, as there are more sedimentary units than basalts in the subsurface, four of which include gravel. The increase in sedimentary units is probably due to this location being closer to the center of the Big Lost drainage than other wells in the TRA well field.

Fence diagram E-E' (Figure A-6) follows a rather tortuous route that starts at USGS-80 and ends at TRA-6A. It is the first traverse to include both geochronological control wells USGS-80 and TRA-5A, and also one of the deepest wells at INL, TRA-5. The flow break in the middle of basalt TRA-B3, which can be seen on the geophysical logs, is not present in the stratigraphic column for TRA-5A. It is likely present in the subsurface, but since there are no geophysical logs for TRA-5A, we can only postulate that the flow break exists. We cannot place it, however, on the stratigraphic column for this borehole since we currently have no data as to what depth it might occur. Basalt TRA-B3 and TRA-B4 thicken and slightly deepen toward the southwest in comparison to TRA-B6, assumed here to be the same as the "AEC Butte basalt," which loses 50 ft of elevation over less than one third of a mile. Basalt TRA-B7 is dated at 786 ± 23 ka on a core from borehole TRA-5A. This is pertinent, since on this fence diagram we can compare the USGS's position for the "I-Flow," which is equated with the basalt of AEC Butte in the current versions of the USGS groundwater model for INL. It is obvious that the I-Flow position deepens to the southwest much more steeply than TRA-B6. In the USGS groundwater model, the I-Flow is considered to be a relatively impermeable unit. In TRA-6A, USGS-65, TRA-5, and USGS-58, the top of the I-Flow coincides to "cinder" bearing intertrappean layers. In Well USGS-58, the units corresponding to the USGS I-Flow interval are more suggestive of near-vent facies than massive coherent basalt. The USGS I-Flow is discussed in detail later in this report.

Fence diagram E-E' also shows that the basalt TRA-B5 (brown) and intertrappean layer TRA-I5 work their way into the stratigraphy from the southwest. The contact between TRA-B7 and TRA-B8 resembles a flow break in the eastern half of the TRA well field that becomes more prominent toward the west. Between USGS-65 and TRA-6A (two wells that are only ~50 ft apart) basalt TRA-B7 pinches out and an intertrappean layer of cinders and clay pinches in. Basalt TRA-B8 is seen to be thickest to the north and thins out to the south. The empty triangle symbols beside the stratigraphic columns for wells USGS-54 and USGS-55 mark the location of a perched water layer encountered during the construction of these wells in the late 1950s.

If the stratigraphic sequence presented here is correct, then any geochemical data for subsurface basalts should confirm this hypothesized stratigraphic order. Geochemical analyses were performed on sample cores from the two geochronological control locations, USGS-80 and TRA-5A. Figure 4-2 presents geochemical results for USGS-80 and TRA-5A graphically, while Table 4-3 presents the data in tabular form. The data used here are from the ISU ESRP geochemisrty database (Hughes, McCurry, and Geist 2002; Reed, Bartholomay, and Hughes 1997; Hughes and McCurry 2002[g]). The match of geochemical data for these two locations is generally good, with the exception of some anomalous results at the very top of basalt TRA-B6 (the AEC basalt) from borehole TRA-5A.

Fence diagram F-F' (Figure A-7) shows a traverse similar to A-A' (Figure A-2), with USGS-80 on the eastern end but ending at TRA-7 instead of TRA-6A. This is also the second traverse to include both USGS-80 and TRA-5A, which provide geochronological control for the TRA well field. This fence diagram shows several features that are absent on A-A', which does not extend as far west. Basalt TRA-B1 pinches out to the west, as do TRA-B2, TRA-B4, and intertrappean layer TRA-I3 (red). Basalt TRA-B5 and the intertrappean layers above and below it come in from the west and pinch out to the east somewhere under Monroe Boulevard. Basalts TRA-B6, -B7, and -B8, which are prominent in the eastern part of the well field, cannot be correlated in the geophysical logs and lithology of TRA-7. This is one of the few places where the basalt TRA-B3 includes some sediment at the position of its central flow break, but only in Well TRA-7.

Fence diagram G-G' (Figure A-8) shows a traverse through boreholes and wells just to the south of F-F', constructed to see if basalts TRA-B6, -B7 and -B8 can be correlated in these wells—an attempt that did not succeed with the data currently available. This is also a diagram that helps to confirm the order of the shallow basalts, TRA-B1 and -B2, based on position only, without relying on just one inclination data point from USGS-80 (see the discussion on A-A' above). Again, there are sediments at the position of the central flow break in TRA-B3 in Well TRA-7 but these are absent in TRA-8. The implication here is that either TRA-B3 is a composite basalt, or it is two or more individual flows.

Fence diagram H-H' (Figure A-9) slices from the northern edge of the TRA well field to the western edge, from Well TRA-2 to USGS-66. This diagram shows again that basalt units common in the eastern half of the well field do not persist to the western edge of the field. It does show, however, that deep sediments can be correlated even when shallow correlations disappear. Well TRA-2 is problematic, however, which is better demonstrated on the next fence diagram. Well TRA-2 is a well with a lithological log but no geophysical logs. These circumstances make it very difficult to correlate this well with its neighbors, and any attempts to do so lack the confidence of other correlations in the TRA well field.

Fence diagram I-I' (Figure A-10) is a traverse through the northernmost wells in the TRA well field that is bounded to the north by the line of vents including AEC Butte. If AEC Butte is the last and highest part of a shield volcano, which is now buried in the subsurface by younger basalts, then we should see the AEC Butte basalt (TRA-B6) in a shallow position in the wells closest to the butte and in a deeper position in Site-19, the well furthest from the butte. Given the data available for this traverse (i.e., mainly lithological and geophysical logs 40 to 50 years old), basalt TRA-B6 cannot be found in the wells northwest of USGS-80, though basalts TRA-B2 and -B3 are present. The dip in these units between MTR-Test and TRA-4 is real and not at all surprising since pahoehoe surfaces can undulate as much as 50 ft normally and up to 100 ft in extreme cases. There is a general trend of deepening units, especially below ~4,750 ft MSL, between MTR-Test and Site-19, even if TRA-B6 cannot be identified this far west.

---

g. S. Hughes and M. McCurry, 2002, ISU geochemistry database, unpublished data, December 2002.

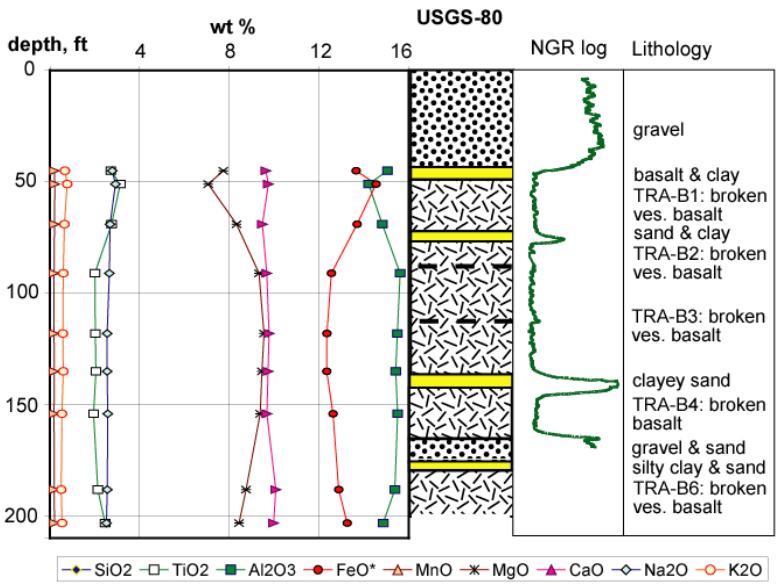

a. Geochemical profile of USGS-80 showing concentrations of eight major element oxides as weight percents.

NOTE: *From left to right are shown the concentration curves, a stratigraphic column, the natural gamma log and descriptive lithology. The natural gamma data and lithology are from Chase et al. (1964). For comparison purposes, TRA-B1 occurs in USGS-80 but not in TRA-5A. All other basalt units are common to both locations. It is likely that the TRA-B2 interval was missed when samples were collected for geochemical analyses.*

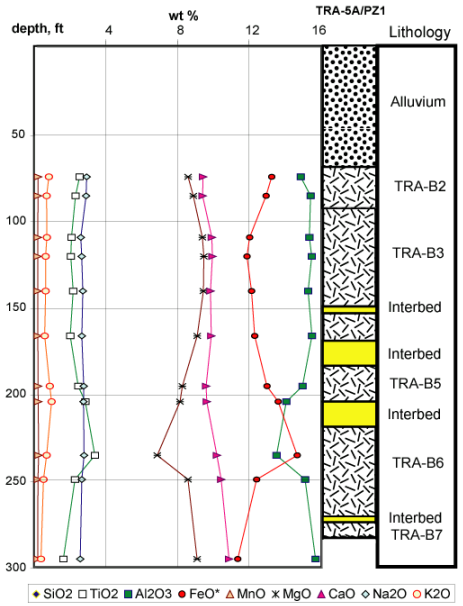

b. Geochemical profile of TRA-5A.

NOTE: *This profile shows concentrations of eight major element oxides as weight percents. From left to right are shown the abundance curves, a stratigraphic column, and descriptive lithology. TRA-5A was a failed borehole that was abandoned during drilling. No geophysical logs were collected. Flow contacts are from Champion et al. (2002). Lithology is based on an unpublished log that is based on cores (Champion 2002[h]). Stratigraphic assignments are based on this study. For comparison purposes, TRA-B2 occurs in TRA-5A but might not have been sampled in USGS-80. Basalts TRA-B5 and TRA-B7 occur here but not in USGS-80. All other basalt units are common to both locations. Overall, the geochemical data for the basalts common to both locations match. The anomalous data in the upper part of TRA-B6 might be an unidentified flow unit distinct from basalt TRA-B6.*

NOTE: *These two profiles are good examples of the value of geochemical data for stratigraphic correlation purposes, especially with the good data match of basalt TRA-B3, the thickest basalt at both locations. Dotted layers are sedimentary layers containing gravels. Yellow layers are sediments with no identified or logged gravels. Stippled areas are basalt. Horizontal solid lines are flow breaks, while horizontal dashed lines are inferred flow breaks.*

Figure 4-2. Geochemical profiles of USGS-80 and TRA-5A.

h. Champion, D., USGS, personal communication to S. Ansley, INL, May 2002.

Table 4-3. Major element geochemical data for Well USGS-80 and Borehole TRA-5A.

Well	Elev. (ft)	Depth (ft)	Depth (m)	SiO2	TiO2	Al2O3	FeO*	MgO	CaO	Na2O	K2O
USGS-80											
	4,898	45	13.7	47.0	2.71	15.1	13.7	7.73	9.6	2.78	0.67
	4,896	51	15.5	47.4	3.14	14.2	14.5	7.06	9.7	2.92	0.77
	4,891	69	21.0	46.8	2.75	14.8	13.7	8.32	9.5	2.68	0.64
	4,884	91	27.7	47.0	2.00	15.6	12.6	9.32	9.7	2.65	0.59
	4,876	118	36.0	47.1	2.03	15.5	12.3	9.54	9.8	2.55	0.57
	4,871	135	41.1	47.3	2.05	15.4	12.3	9.45	9.7	2.55	0.59
	4,865	154	46.9	47.2	1.94	15.5	12.6	9.38	9.7	2.57	0.53
	4,855	188	57.3	47.1	2.13	15.4	12.9	8.74	10.1	2.55	0.50
	4,850	203	61.9	47.2	2.46	14.9	13.3	8.44	10.0	2.52	0.54
	Source: 1996 data, ISU Geochemistry Lab.										
TRA-5A											
	4,853	74	22.6	46.9	2.52	14.9	13.3	8.59	9.4	2.91	0.81
	4,842	85	25.9	46.8	2.30	15.4	12.9	8.88	9.4	2.88	0.68
	4,818	109	33.2	47.3	2.07	15.4	12.0	9.39	9.9	2.59	0.69
	4,807	120	36.6	47.3	2.03	15.5	11.9	9.47	9.9	2.64	0.62
	4,787	140	42.7	47.2	2.16	15.3	12.1	9.45	9.8	2.70	0.62
	4,761	166	50.6	47.4	2.00	15.5	12.3	9.09	9.9	2.65	0.57
	4,732	195	59.4	47.3	2.44	15.0	13.0	8.27	9.6	2.75	0.85
	4,723	204	62.2	47.1	2.84	14.1	13.6	8.14	9.6	2.74	0.96
	4,692	235	71.6	47.0	3.38	13.5	14.7	6.86	10.2	2.77	0.68
	4,678	249	75.9	47.4	2.26	15.1	12.4	8.58	10.4	2.65	0.51
	4,632	295	89.9	47.9	1.62	15.7	11.4	9.09	10.9	2.56	0.37
	Source: 1997 data, ISU Geochemistry Lab.										

* Total iron reported as FeO.

NOTE: *Data is from the ISU ESRP geochemistry database.*

Well TRA-2 presents difficulties for correlations between MTR-Test and Site-19. If TRA-2 is removed, the correlations between Site-19 and TRA-4 improve in its absence. The problem with TRA-2 is its lithological log, which is the only dataset available for this well. The lithological and geophysical logs for Site-19 and TRA-4 reveal a detailed stratigraphy, especially between 4,700 and 4,300 ft MSL. In comparison, the lithological log for TRA-2 lacks these details. It is for this reason that units with correlations between TRA-4 and Site-19 are not carried through the stratigraphic column for TRA-2 on the diagram.

4.2.1 Correlating Middle-1823 within the TRA Well Field

Cross section J-J' (Figure A-11) is a north-south transect from Site-19 at the northwest corner of TRA to ICPP-SCI-V-214 at the Vadose Zone Research Park (VZRP). The local stratigraphy seen in this cross section is relatively flat. In general, correlations are more difficult to establish along the western edge of the TRA well field. Despite this, basalts TRA-B3 (light green in the figure) and TRA-B5 (brown) are present in at least five locations each. Basalts TRA-B3 and -B4 (dark green) are found in both Site-19 and USGS-79. Basalt TRA-B4 pinches out to the south of USGS-79, but TRA-B3 persists as far south as Middle-1823. TRA-B3 might actually be present in ICPP-SCI-V-213 and -214 since a basalt in the equivalent stratigraphic position in ICPP-SCI-V-214 has an inclination of 77.4°±1.2°. This is a close match to basalt TRA-B3 in borehole TRA-5A at 76.6°±1.2° and in Well USGS-80 at 74.9°±3.2°. The

hesitation for extending TRA-B3 as far south as the VZRP is based on the change in character seen in Middle-1823. In Middle-1823, this basalt is much more disturbed than elsewhere, including zones of no recovery and infiltration of clay into the lower portions of the unit. This is sufficiently different from the basalts in ICPP-SCI-V-213 and -214, and a correlation between the two really demands more data than what is currently available. Duane Champion from the USGS has sampled Middle-1823 for paleomagnetic studies. Unfortunately, a paleomagnetic inclination at the level for TRA-B3 in this well, which might have helped to confirm or refute that the presence of TRA-B3 at the VZRP is not possible since the interval from 0 to 500 ft bls in Middle-1823 was not cored.

Basalt TRA-B5 along with the clayey interbeds TRA-I4 and TRA-I5 above and below it, respectively, can be correlated from USGS-79 south to ICPP-SCI-V-213. In addition, a set of sediment layers between 4,600 and 4,650 ft MSL occur in Middle-1823 and the wells of the VZRP. A similar situation exists for a sandy clayey interbed found between 4,200 and 4,250 ft MSL in Wells Site-19, USGS-79, and Middle-1823. These are only a few of the correlations that might exist along this cross section, but others cannot be identified or inferred with the data currently available.

Cross section K-K' (Figure A-12) follows a transect from Middle-1823 northeastward to MTR-Test. Basalts TRA-B1 and -B2 both appear to pinch out to the southwest and never make it as far as Middle-1823. It is possible, however, that paleomagnetic inclinations for the Middle-1823 basalts above TRA-B3 will match the inclinations of TRA-B1 and -B2, and establish correlations for this well that are unexpected based on differences seen in the lithological logs. As seen already in cross section J-J' (Figure A-11), TRA-B3, TRA-I4, TRA-B5, and TRA-I5 form a suite of units present in most of the western wells in the well field, including Middle-1823. The other notable feature of this cross section is the correlation of sediment layers between Middle-1823 and TRA-5 at 4,000 ft MSL and deeper. These correlations are based on lithology and geophysical logs without input from paleomagnetic inclinations or radiometric age dates, which are rare in strata this deep at INL.

Cross section L-L' (Figure A-13) is parallel and displaced to the east of cross section K-K' (Figure A-12). Basalt TRA-B5 is not present, which supports the constraint that TRA-B5 is found only along the western edge of the well field. TRA-B4 is seen on the north end of the section but pinches out to the south before it could reach Well USGS-76. The clayey intertrappean layer TRA-I3 is present under basalt TRA-B3 in every well deep enough to penetrate it. Again, basalt TRA-B3 is present in all the wells along the cross section. Like in Wells Middle-1823 and TRA-7, the TRA-B3 basalt is somewhat disturbed and in Well USGS-76 hosts a distinct layer of intertrappean sediments at the position of its central flow break. Whether these clayey sediments were bedded or placed by infiltration is not known. Overall, most of the basalt and intertrappean units found in the northeast portions of the TRA well field do not persist south as far as Well USGS-84.

4.3 Identified Units of the Test Reactor Area Well Field

The following subsections provide information regarding stratigraphy of identified units within the TRA well field.

4.3.1 Basalt Unit TRA-B1

Basalt Unit TRA-B1, age 419 ± 33 ka, is a grey basalt ~30 ft thick or less, often logged in the field as vesicular and/or broken. It occurs typically between elevations of 4,850 and 4,900 ft MSL (see Table 3-1). It can be correlated in boreholes along and parallel to Monroe Boulevard from Well USGS-66 to the southeast corner of TRA. To the west and southwest, in Wells Site-19, USGS-79, TRA-6A, TRA-7 and TRA-8, its stratigraphic position is occupied by a thicker sequence of black and grey broken basalts, often finely interbedded or infiltrated with clayey sediments. The extent of TRA-B1 to the north and east

is unknown, though it cannot be correlated by position in any INTEC wells to the east. Its expected position in Well MTR-Test is occupied by a 20-ft yellow silt (possibly loess). To the west of MTR-Test, it is possible that the grey and brown, broken-or-soft basalt in Wells TRA-2, TRA-4, USGS-72, and USGS-68 belongs to TRA-B1, but this cannot be determined with certainty based on the information currently available for these four wells. The lack of any wireline logs for TRA-2 is particularly unfortunate in this case.

Age control for TRA-B1 is provided by a date of 419 ± 33 ka on core from Well USGS-80. To the east, the nearest chronological-control well to USGS-80 is Well USGS-121. A date of 77 ± 39 ka exists for the interval between 4,900 and 4,850 ft MSL in Well USGS-121, which obviously does not correlate with TRA-B1. An interval of bedded vesicular basalt in USGS-121 at ~4,700 ft elevation has an average normal inclination of ~55°. This inclination is bracketed between USGS-121 age dates 376 ka @>134 ft bls and 543 ka @324 ft bls, and is within the confidence limits for the inclination of TRA-B1 in USGS-80 of 54.5° ± 1.3°. Based on the match between the inclinations, it is possible that the basalt sequence in USGS-121 at ~4,700 ft MSL correlates in time with TRA-B1 in USGS-80. If so, then there is a depth difference of ~150 ft between them, a significant though not prohibitive discrepancy. Of geochemistry samples collected from the USGS-80 core, the first three samples are from TRA-B1. Only one geochemical sample was analyzed in the potentially corresponding interval in USGS-121, at ~4,701 ft MSL. Geochemically, the USGS-121 sample from ~4,701 ft MSL most closely resembles the second and third USGS-80 samples from basalt TRA-B1, but the match is not adequate since calcium, phosphorus, and uranium concentrations were sufficiently different. In general, it is not advisable to stretch the geochemical data to force a correlation based on just one sample interval in USGS-121. Analyses from several intervals immediately above and below the ~4,701-ft MSL location would provide a more robust amount of data adequate for comparison. This is one of several examples where sampling interval variations in the ISU geochemistry database hampers our ability to use this data to clarify stratigraphic correlations.

The source of TRA-B1 is not known, though the most likely general direction of this basalt's vent is to the north, since this flow cannot be correlated to the west or south. Basalt TRA-B1 is likely not the same as the basalt from the ~4,700 ft MSL interval in USGS-121, so a source to the east can be ruled out as well. The 626 ka AEC Butte (Qv1) is too old to be the source, and the 337 ka vent immediately to the west of AEC Butte (Qv2) is too young.

4.3.2 Intertrappean Layer TRA-I1, between TRA-B1 and TRA-B2

Basalt TRA-B1 is commonly separated from TRA-B2 below it by a thin intertrappean layer most often described as "basalt and cinders," though sometimes as "cinders and sand" or "cinders and clay." This cindery intertrappean layer—TRA-I1—does not always occur in wells with both TRA-B1 and TRA-B2; for example, it is absent in Wells USGS-60, USGS-61, USGS-64, USGS-68 and USGS-70. There appears to be no common factor involved in wells where TRA-I1 is missing.

4.3.3 Basalt Unit TRA-B2

Basalt Unit TRA-B2 has an age between 419 ka and 461 ka. TRA-B2 is a thin grey basalt, sometimes described as broken, which resembles TRA-B1 in almost every respect. It occurs in the interval between 4,850 and 4,825 ft MSL elevation. Basalt Unit TRA-B2 extends slightly more to the south and west when compared to TRA-B1, though it too cannot be correlated by position to the east, south, and west. Geochemically, it most closely resembles the basalt at ~4,700 ft MSL in Well USGS-121, but their paleomagnetic inclinations (55° vs. 67°) are too different to argue that a correlation exists between them (see Table 3-1).

4.3.4 Intertrappean Layer TRA-I2 between TRA-B2 and TRA-B3

Basalt TRA-B3 is separated from TRA-B2 by a discontinuous layer described as cinders, or as basalt and cinders. To the south of TRA and Monroe Boulevard, there is no intertrappean material between Units TRA-B2 and TRA-B3. To the east of the TRA compound, the TRA-I2 layer is typically between 5 and 10 ft thick. It appears to thicken to the west, where it reaches its maximum thickness of 30 ft at Site-19. To the southwest, in TRA-7 and TRA-8, there is a sandy silt in the equivalent position to the cindery TRA-I2. It cannot be determined with the data on hand, however, if this sandy silt correlates to TRA-I2 with the cinders removed (i.e., whether TRA-I2 is really a sandy silt that acquired a cindery component near a volcanic vent that was active while the silt was deposited).

The problem with correlating layers with "cinders" should be kept in mind when evaluating TRA-I2. Layer TRA-I2 is not present in USGS-80, so we cannot inspect core to see if the cinders in this layer are cinders *sensu stricto* or "cinders" in the more general sense as described in Chase et al. (1964).

4.3.5 Basalt Unit TRA-B3

This unit has pooled age data of 414 ± 8 ka (Champion et al. 2002), and a USGS-80 age date of 461 ± 24 ka (Lanphere, Champion, and Kuntz 1993). Basalt Unit TRA-B3 is the thickest, most widespread basalt in the TRA environs and the most complex. It is the first unit in the TRA well field that can be correlated in Middle-1823, as well as in boreholes closer to TRA itself. In 12 of 28 boreholes that penetrate it, TRA-B3 is a 40- to 75-ft-thick unit of grey basalt that is likely two or more distinct flows with at least one prominent break between flows at ~4,800 ft MSL. This flow break effectively bifurcates the unit into upper and lower portions. In Wells TRA-7 and USGS-76, this flow break hosts a thin layer of sand/silt or clay, respectively. Since sediment infiltration is not uncommon in basalts of the ESRP, it is not unreasonable for these sediments to be infiltrated loess. Without a better description of these sediments, however, it is not possible to determine if these are infiltrated or deposited sediments. If we knew this, we could then evaluate if the upper and lower TRA-B3 basalts were two different and distinct flows with similar inclinations or one flow group with two related flow units. The three TRA-B3 geochemistry samples suggest that this unit is one flow group with two or more flow units.

As a thick, two- or three-part flow group, TRA-B3 occurs in the wells and boreholes that penetrate the flood plain of the river or in wells that lie very close to the flood plain's northwest edge. Well Middle-1823 is one of these boreholes. These boreholes also include the two that establish chronological control for this unit, Well USGS-80 and borehole TRA-5A/PZ1 (see Table 3-1). The inclinations of TRA-B3 in these two boreholes are 74.9° ± 3.5° and 76.6° ± 1.2° respectively. Champion et al. (2002) assigned a pooled age of 414 ± 8 ka to TRA-B3. This date is significantly different from the original age of 461 ka for USGS-80 alone (Lanphere, Champion, and Kuntz 1993).

This pooled younger age of 414 ka is problematic in that it implies that TRA-B3 is as young or younger than basalt TRA-B1, which lies stratigraphically above it. A comparison of intervals of similar age (~441 ka to ~466 ka) from nearby wells (USGS-121, USGS-123, and WO-2) does not clarify this situation. None of the intervals compared are similar enough in geochemistry to argue that they were erupted at the same time and/or shared the same source. It is unfortunate that there are no geophysical or detailed lithological logs for the chronological-control borehole TRA-5A/PZ, since this borehole was abandoned during drilling.

In several wells west of TRA proper, along the north edge of TRA inside the fence or along the most eastern edge of the TRA well field, basalts correlated as part of Unit TRA-B3 lack the bifurcating flow break dividing the basalt into upper and lower portions and are usually approximately half the thickness of the multiflow unit in the center of the TRA well field discussed above. Where TRA-B3 occurs in the wells west of TRA proper, it appears that only the top half of the unit can be correlated with

any confidence. In the wells along the north TRA fence (TRA-2 to MTR-Test), it is possible that basalt assigned to the next lower unit (TRA-B4) is actually miscorrelated and is really the presumed-missing bottom portion of TRA-B3 separated by a layer of "cinders," though shape matching of the NGR logs for Site-19, TRA-4, and MTR-Test argues against this potential interpretation. The western half of the Site-19 to MTR-Test-to-USGS-80 cross section is perhaps one of the most difficult to correlate since there are no wireline logs available for TRA-2, only a geologist's log that is over 50 years old. For the most easterly wells—USGS-66, USGS-62, and USGS-71—the top portion of the multiflow TRA-B3 unit matches, but the bottom portion has been replaced by a sequence of thinly bedded cinders, clay, and basalt.

Basalt TRA-B3 could occur as far south as the VZRP. Well ICPP-SCI-V-214 includes a basalt with an inclination of 77.4° ± 1.2° at the depth we would expect to find TRA-B3, ~4,800 to ~4,780 ft MSL. The occurrence of TRA-B3 at Middle-1823 is inferred with less confidence than its correlation in wells to the north. It is regrettable that core could not be collected in the upper 500 ft of Middle-1823, because a high 70°s paleomagnetic inclination measurement for TRA-B3 at this location would allow both the correlation of this basalt with confidence in Middle-1823 and an inferred correlation for it in ICPP-SCI-V-213 and -214.

4.3.6 Intertrappean Layer TRA-I3, between TRA-B3 and TRA-B4

Basalt TRA-B4 is separated from TRA-B3 by a coherent and mostly continuous layer, which has a cinder and/or clay component almost without exception. It is usually 5 to 15 ft thick, although it is thicker to the west. It can be as thin as 2 ft in TRA-5A and as thick as 30 ft in USGS-72. It occurs as far south as USGS-84 and also occurs in almost all the wells in the northern half of the well field. It is absent in the westernmost wells from TRA-7 to the VZRP. It also is absent from USGS-39. Its existence throughout most of the well field argues that TRA-B3 was not erupted closely in time after basalt TRA-B4 since this layer, with its fine-grained sedimentary component, had enough time to develop and deposit.

4.3.7 Basalt Unit TRA-B4

Basalt Unit TRA-B4 has an age between 461 ka and 643 ka. This unit often lacks a description other than "basalt," though in the places where more information is available it is labeled as a grey or brown basalt, sometimes broken. It is usually 15 to 30 ft thick and occurs only in the northern half of the TRA well field. It might actually continue eastward, though it cannot be identified with confidence in the easternmost well, USGS-66, because of the pinching in and out of basalts and interbed units going from USGS-58 to USGS-62 to USGS-66. TRA-B4 has a paleomagnetic inclination of 59.6° ± 5.8° in USGS-80, and 58.4° ± 3.6° in TRA-5A. There is no age date for this flow, but it is sandwiched by the 461 ka TRA-B3 above and the 643 ka TRA-B6 below.

4.3.8 Intertrappean Layer TRA-I4, between TRA-B4 and TRA-B5

Basalt TRA-B5 is overlain and separated from TRA-B4 by an interbed, TRA-I4, made up of variable sediment types. The description of these sediments excludes any cinders without exception. In some places, two or more different sediments are lumped together under the descriptor of TRA-I4, and these are usually distinguished on the fence diagrams and cross sections. It can be an interbed as thin as 10 ft and as thick as 50 ft. It only occurs in seven boreholes or wells in the western third of the well field. On the strength of position and lithological description, TRA-I4 is inferred in Well ICPP-SCA-V-213 at 4,770 to 4,735 ft MSL.

It is better to think of this layer as overlaying the basalt TRA-B5, which also tends to the western half of the well field rather than being below basalt TRA-B4. Layer TRA-I4 appears under TRA-B4 in only three out of eleven TRA-B4 borehole locations. It appears underneath TRA-B3 more often than it

does under TRA-B4. In these cases, it is usually distinguished from TRA-I3 by its lack of "cinders." In reality, TRA-I4 is likely several different sediments from multiple sources, all of which probably have origins to the west.

4.3.9 Basalt Unit TRA-B5

Basalt Unit TRA-B5 has an age between 461 ka and 643 ka. Basalt TRA-B5 occurs in wells or boreholes in the western half of the well field, from USGS-79 to ICPP-SCI-213. It is described as a dark grey or black basalt, 20 to 30 ft thick. It has a paleomagnetic inclination of 72.2° ± 0.9° in ICPP-SCI-V-213, and 74.0° ± 2.4° in TRA-5A.

4.3.10 Intertrappean Layer TRA-I5, between TRA-B5 and TRA-B6

Layer TRA-I5 is an interbed of mixed sand or silty sand and clay. It is usually ~15 ft thick though it can vary from as thin as 5 ft to as thick as 25 ft. It only occurs in seven boreholes or wells in the western third of the well field, and always underneath TRA-B5. Basalt TRA-B6 occurs underneath this interbed in only two locations, TRA-5A and USGS-65/TRA-6A.

4.3.11 Basalt Unit TRA-B6

Basalt Unit TRA-B6 has pooled age data of 637 ± 35 ka (Champion et al. 2002), a USGS-80 age date of 643 ± 64 ka (Lanphere et al. 1993), and AEC Butte age of 626 ± 67 ka (Champion, Lanphere, and Kuntz 1988).

Although this basalt occurs in only six locations, TRA-B6 is the most important shallow basalt in the TRA well field. Due to its thickness, complexity, and large subaerial extent, basalt TRA-B3 has valid claims as an important unit in the TRA volcanostratigraphy; however, the stratigraphic correlations between TRA and INTEC hinge on TRA-B6. In subaerial extent, TRA-B6 occurs on either side of Monroe Boulevard. It is a grey basalt, 40 to 50 ft thick. In USGS-80 and USGS-58, it is described as being broken. It probably is a flow group, not a single flow unit, because up to three flow breaks can be observed in the geophysical logs.

Basalt Unit TRA-B6 has a paleomagnetic inclination of 56.7° ± 0.9° in TRA-5A and 53.9° ± 1.9° in USGS-80. The pooled date of 637 ka is based on the ages of basalts that Champion et al. (2002) has correlated with TRA-5A from AEC Butte, USGS-80, and USGS-123. If we look at geochemical profiles for TRA-B6 and the profile for the 641 ka basalt at ~4,340 to ~4,340 ft MSL in USGS-123, one might make a case that the profiles might be "close enough," except that the behavior of iron in USGS-123 is significantly different. Since iron is one of the six most important elements for geochemically profiling ESRP basalts, its deviation in USGS-123 compared to TRA-B6 is evidence that these could be different units. This supposition coupled with the mismatch of geochemical profiles between TRA-B6 and the basalt of equivalent age in WO-2, it is likely that TRA-B6 does not occur on the INTEC side of the flood plain. If they were the same, then there would be a vertical discrepancy of 400 ft for these units between INTEC and TRA. While a 200-ft vertical discrepency is within the realm of possibility, a 400-ft discrepancy likely cannot be accommodated without invoking some kind of structural disruption.

4.3.12 Units TRA-I6, TRA-B7, TRA-I7, and TRA-B8

Units TRA-I6, TRA-B7, TRA-I7, and TRA-B8 all share approximately the same subaerial extent as TRA-B6. They are much more difficult to correlate because the number of locations where deeper information is available decreases with increasing depth. It is possible that TRA-B7 and TRA-B8 should be combined to form one flow group, but there is not enough information available for these two units to make an informed evaluation. It is also possible that TRA-B7 and/or TRA-B8 should correlate with

basalts along the western edge of the well field. What hinders this, however, is the lack of chronological control at depth. All other dated units in the TRA well field have at least two dates available, but TRA-B7 has only one. This is unfortunate since the date on TRA-B7, 786 ka, is essentially at the Bruhnes-Matayuma transition, a feature we can identify in most of the deep boreholes drilled on-Site because of the characteristic paleomagnetic polarity inversion. If the Bruhnes-Matayuma transition in Middle-1823 is at ~300 ft bls, which is its depth in TRA-5A, then the cores collected for Middle-1823 might be too deep to locate this feature. Figure 4-3 illustrates the correlated units of the TRA well field.

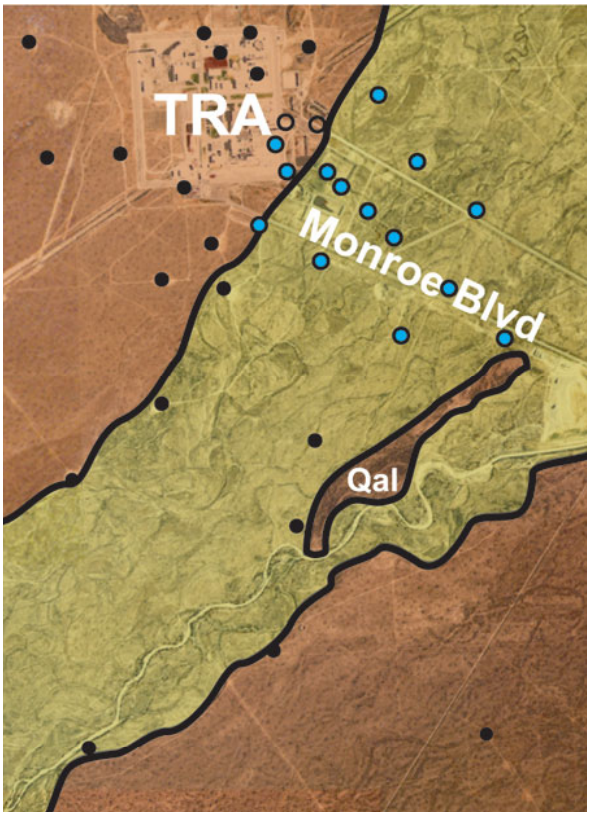

a. The subsurface extent of Basalt Unit TRA-B1.

NOTE: *The maximum and minimum occurrence depths are listed in Table 3-1. In general, this flow varies in thickness between 10 and 30 ft. Solid black circles represent locations where boreholes penetrate deep enough to encounter this unit, but no correlation was found in the appropriate depth interval. Open black circles represent locations where boreholes encountered the top of Unit TRA-B1 but did not penetrate to the bottom of the unit. Solid blue circles with a black rim represent where boreholes encountered flow TRA-B1.*

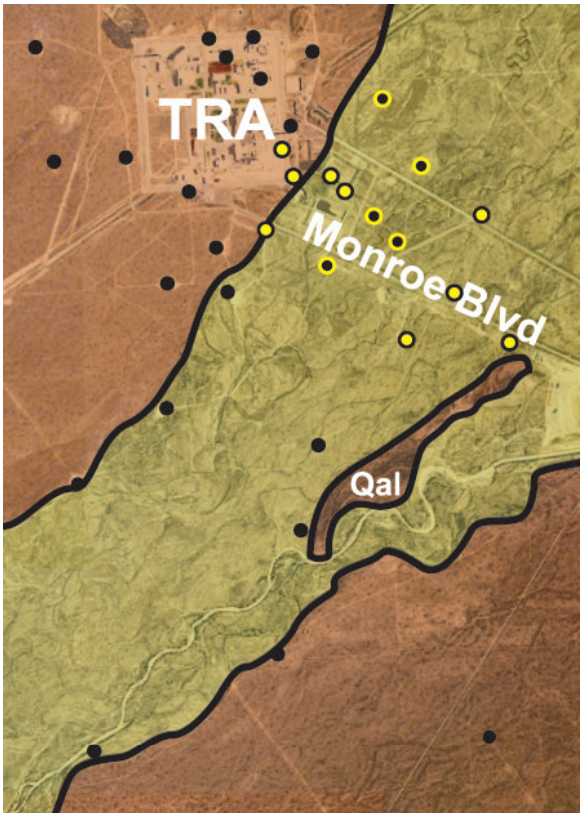

b. The subsurface extent of the intertrappean layer between Basalt Units TRA-B1 and TRA-B2.

NOTE: *Solid black circles represent locations where boreholes are deep enough to penetrate intertrappean material between these two basalt units, but intertrappean material and one or both basalts are absent from the stratigraphic column. Solid black circles with yellow rims represent where basalts TRA-B1 and TRA-B2 are both present in a borehole but no intertrappean material was logged between them. Yellow circles with black rims represent where intertrappean material was logged in the interval between the two basalt units.*

Figure 4-3. Correlated units of the Test Reactor Area well field.

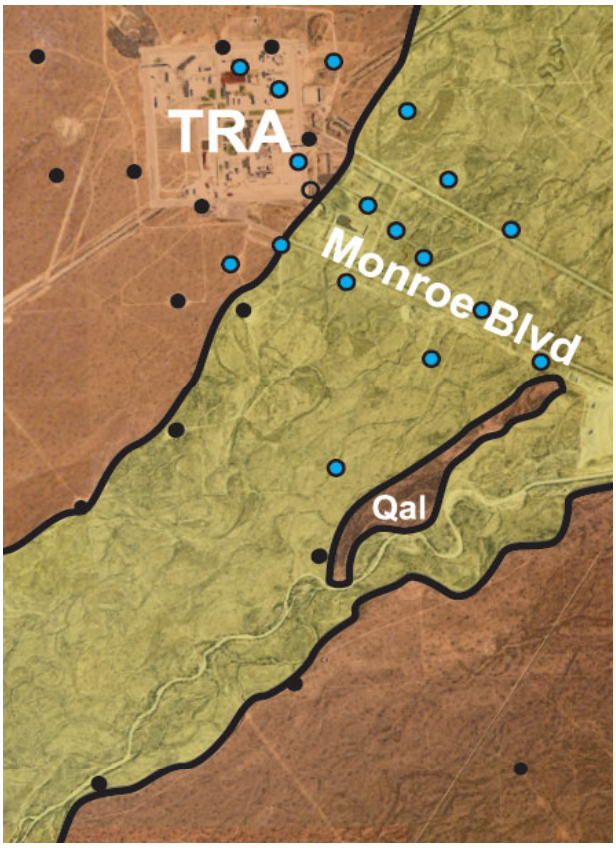

c. The subsurface extent of Basalt Unit TRA-B2.

NOTE: *The maximum and minimum occurrence depths are listed in Table 3-1. In general, this flow varies in thickness between 10 and 25 ft. Solid black circles represent where boreholes penetrate deep enough to encounter this unit, but no correlation was found in the appropriate depth interval. Open black circles represent where boreholes encountered the top of Unit TRA-B1 but did not penetrate to the bottom of the unit. Solid blue circles with a black rim represent where boreholes encountered flow TRA-B1.*

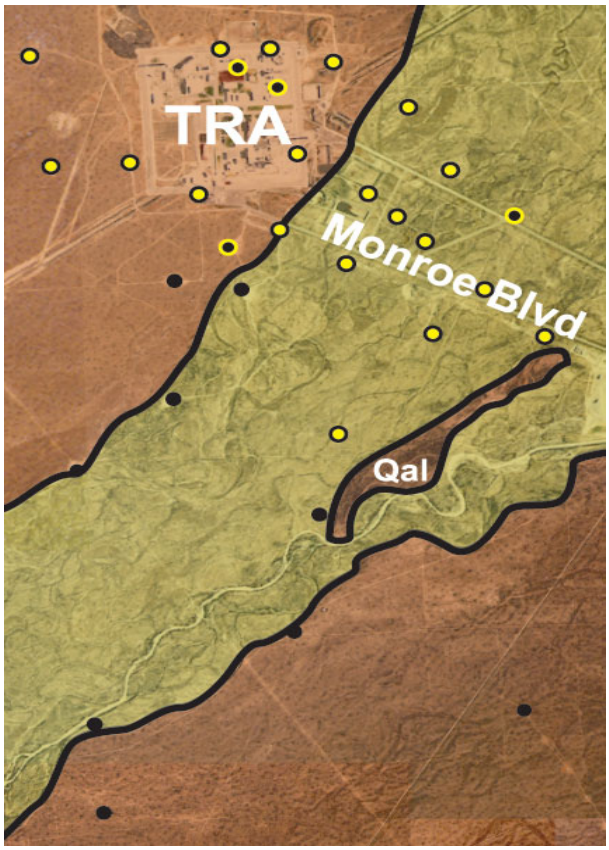

d. The subsurface extent of the intertrappean layer between Basalt Units TRA-B2 and TRA-B3.

NOTE: *Solid black circles represent where boreholes are deep enough to penetrate intertrappean material between these two basalt units, but intertrappean material and one or both basalts are absent from the stratigraphic column. Solid black circles with yellow rims represent where basalts TRA-B2 and TRA-B3 are both present in a borehole but no intertrappean material was logged between them. Yellow circles with black rims represent where intertrappean material was logged in the interval between the two basalt units.*

Figure 4-3. (continued).

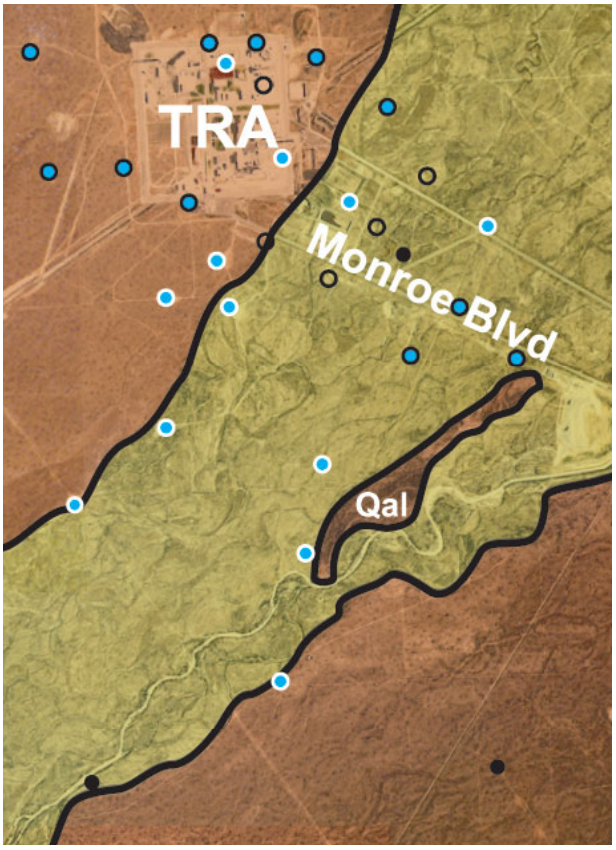

e. The subsurface extent of Basalt Unit TRA-B3.

NOTE: *Basalt Unit TRA-B3 has maximum elevation of ~4,850 ft MSL, and minimum elevation of ~4,750 ft MSL. Solid black circles represent where boreholes penetrate deep enough to encounter this unit but no correlation was found in the appropriate depth interval. Open black circles represent where boreholes encountered the top of Unit TRA-B3 but did not penetrate to the bottom of the unit. Solid blue circles with a white rim represent where boreholes encountered TRA-B3 as a package of two or more flows, with at least one flow break or intertrappean layer at approximately 4,800 ft MSL. Solid blue circles with black rims represent where boreholes penetrated what is interpreted as the upper half of the TRA-B3 flow group.*

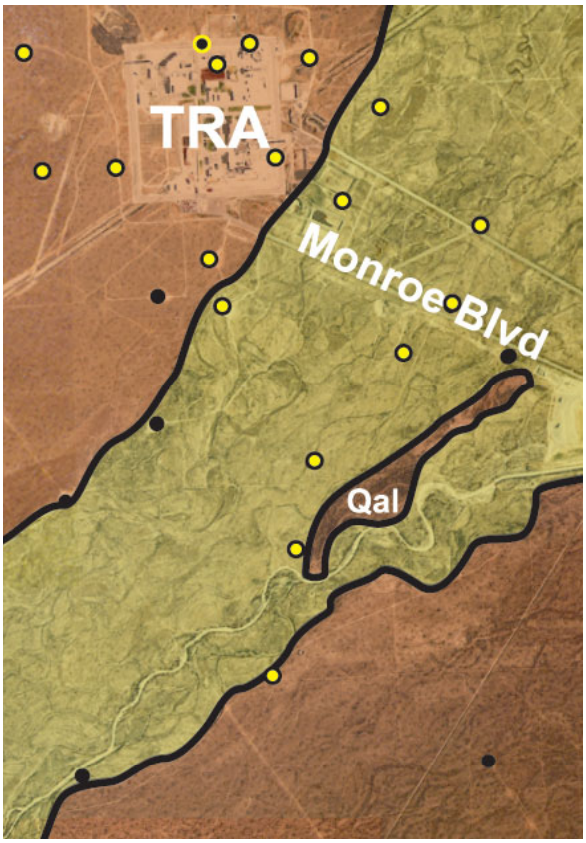

f. The subsurface extent of the intertrappean layer between Basalt Units TRA-B3 and TRA-4.

NOTE: *Solid black circles represent where boreholes are deep enough to penetrate intertrappean material between these two basalt units, but intertrappean material and one or both basalts are absent from the stratigraphic column. Solid black circles with yellow rims represent where basalts TRA-B3 and TRA-B4 are both present in a borehole but no intertrappean material was logged between them. Yellow circles with black rims represent where intertrappean material was logged in the interval between the two basalt units.*

Figure 4-3. (continued).

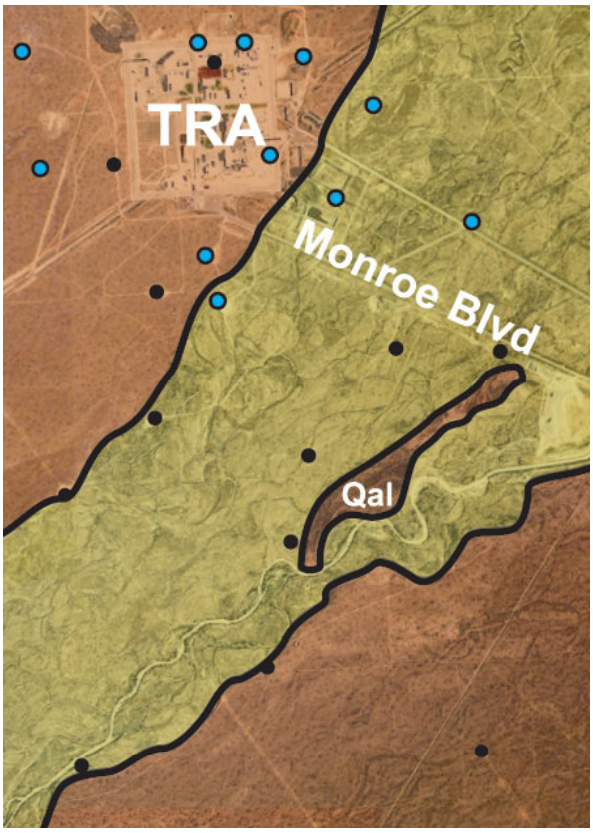

g. The subsurface extent of Basalt Unit TRA-B4.

NOTE: *The maximum and minimum occurrence depths are listed in Table 3-1. In general, this flow varies in thickness between 15 and 30 ft. Solid black circles represent where boreholes penetrate deep enough to encounter this unit, but no correlation was found in the appropriate depth interval. Open black circles represent where boreholes encountered the top of Unit TRA-B4 but did not penetrate to the bottom of the unit. Solid blue circles with black rims represent locations where boreholes penetrated through the TRA-B4 flow group.*

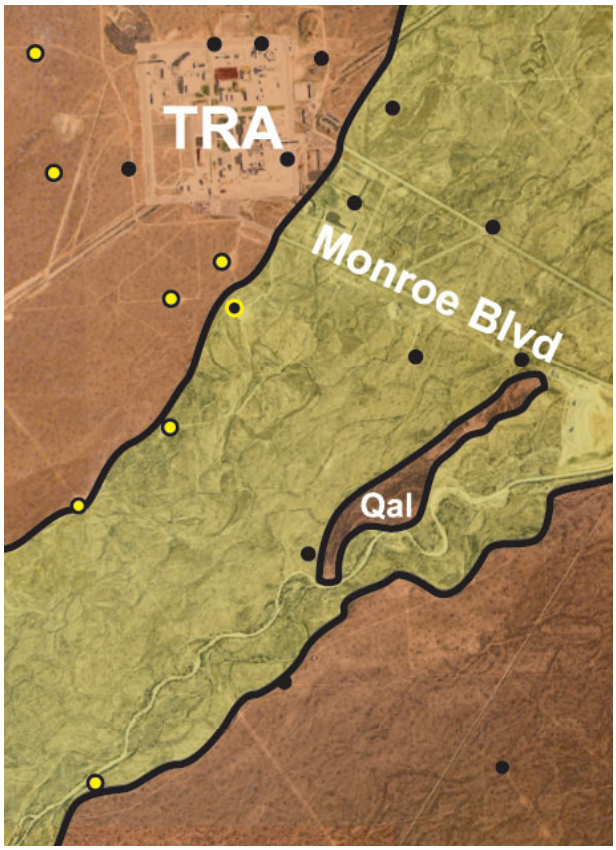

h. The subsurface extent of the intertrappean layer between Basalt Units TRA-B4 and TRA-B5.

NOTE: *Solid black circles represent where boreholes are deep enough to penetrate intertrappean material between these two basalt units, but intertrappean material and one or both basalts are absent from the stratigraphic column. Solid black circles with yellow rims represent where basalts TRA-B4 and TRA-B5 are both present in a borehole but no intertrappean material was logged between them. Yellow circles with black rims represent where intertrappean material was logged in the interval between the two basalt units.*

Figure 4-3. (continued).

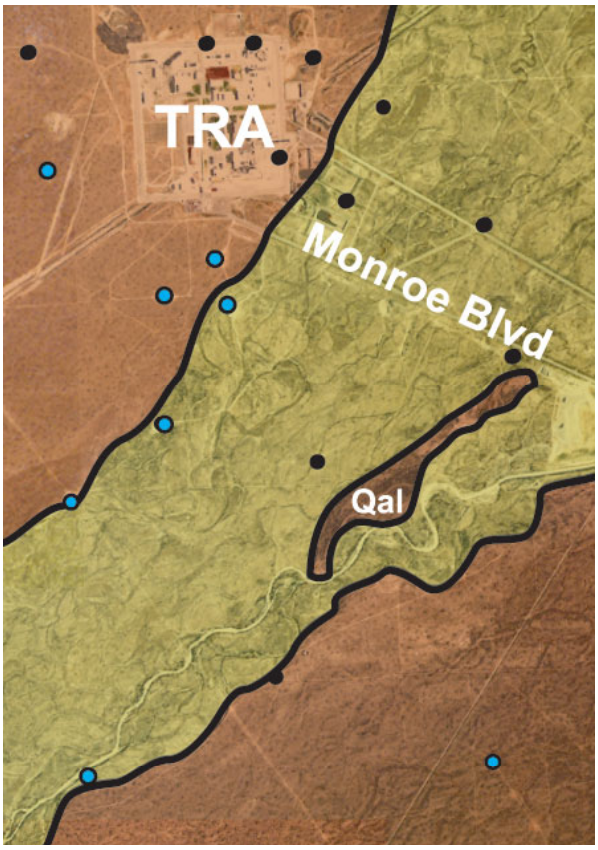

i. The subsurface extent of Basalt Unit TRA-B5.

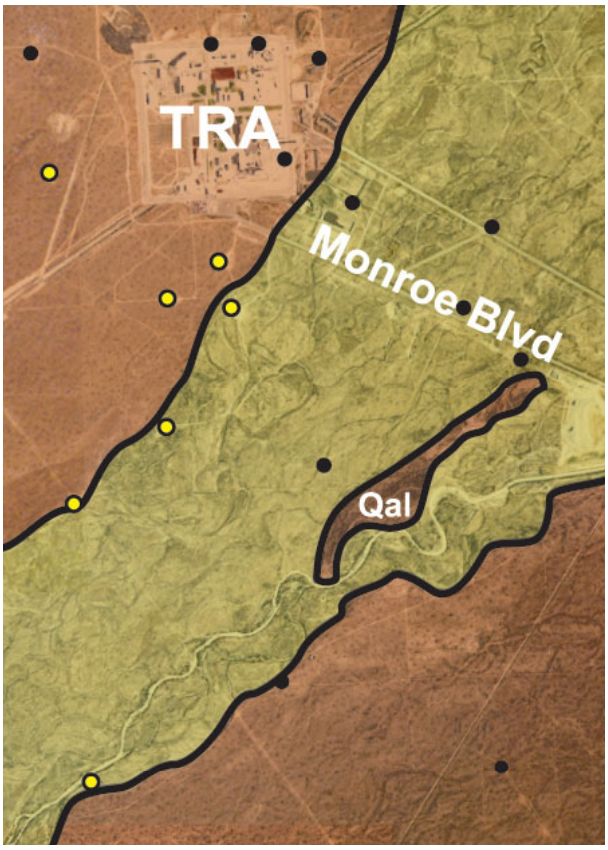

j. The subsurface extent of the intertrappean layer TRA-I5 between Basalt Units TRA-B5 and TRA-B6.

NOTE: *The maximum and minimum occurrence depths are listed in Table 3-1. In general, this flow varies in thickness between 10 and 50 ft. Solid black circles represent where boreholes penetrate deep enough to encounter this unit, but no correlation was found in the appropriate depth interval. Open black circles represent where boreholes encountered the top of Unit TRA-B5, but did not penetrate to the bottom of the unit. Solid blue circles with black rims represent locations where boreholes penetrated through the TRA-B5 flow group.*

NOTE: *Solid black circles represent where boreholes are deep enough to penetrate intertrappean material between these two basalt units, but intertrappean material and one or both basalts are absent from the stratigraphic column. Solid black circles with yellow rims represent where basalts TRA-B5 and TRA-B6 are both present in a borehole but no intertrappean material was logged between them. Yellow circles with black rims represent where intertrappean material was logged in the interval between the two basalt units.*

Figure 4-3. (continued).

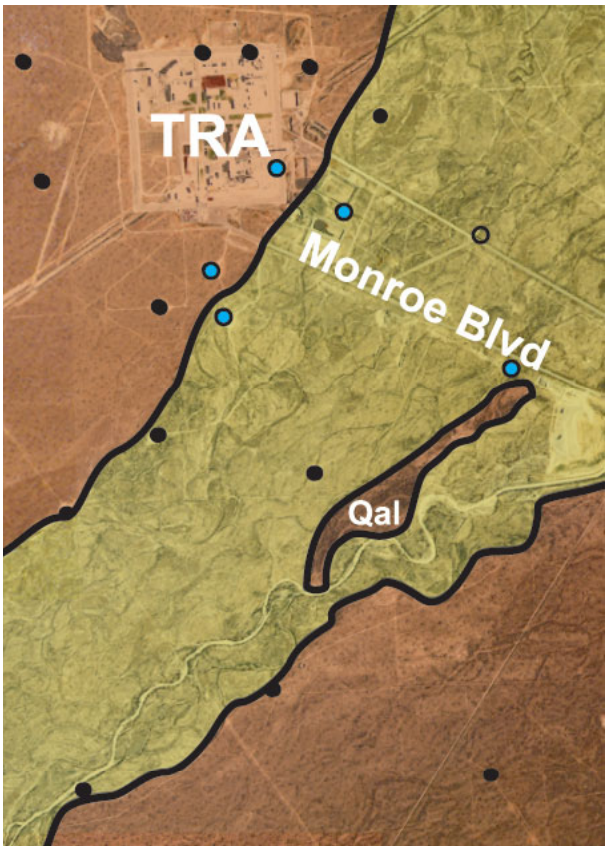

k. The subsurface extent of Basalt Unit TRA-B6.

NOTE: *The maximum and minimum occurrence depths are listed in Table 3-1. In general, this flow varies in thickness between 40 and 50 ft. Solid black circles represent where boreholes penetrate deep enough to encounter this unit, but no correlation was found in the appropriate depth interval. Open black circles represent where boreholes encountered the top of Unit TRA-B6 but did not penetrate to the bottom of the unit. Solid blue circles with black rims represent locations where boreholes penetrated through the TRA-B6 flow group.*

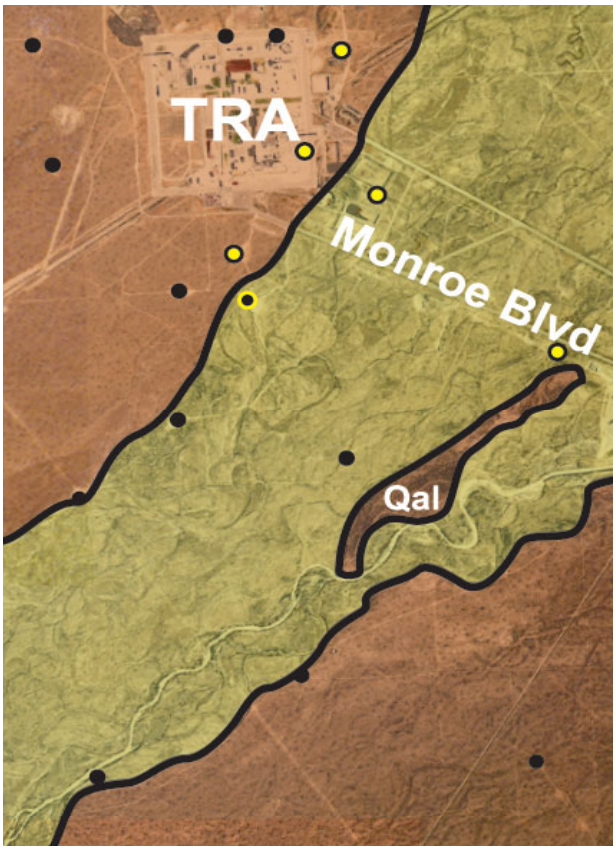

l. The subsurface extent of the intertrappean layer TRA-I6 between Basalt Units TRA-B6 and TRA-B7.

NOTE: *Solid black circles represent where boreholes are deep enough to penetrate intertrappean material between these two basalt units, but intertrappean material and one or both basalts are absent from the stratigraphic column. Solid black circles with yellow rims represent where basalts TRA-B6 and TRA-B7 are both present in a borehole but no intertrappean material was logged between them. Yellow circles with black rims represent where intertrappean material was logged in the interval between the two basalt units.*

Figure 4-3. (continued).

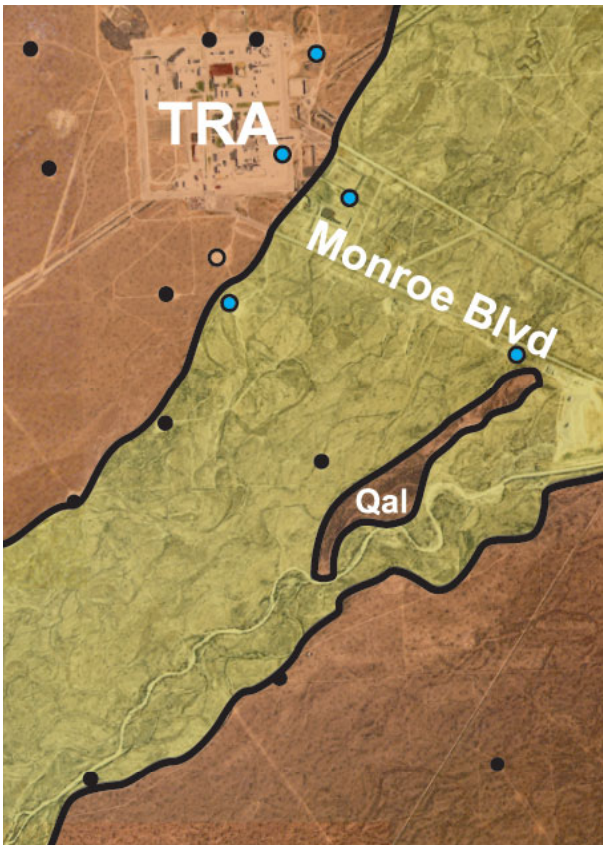

m. The subsurface extent of Basalt Unit TRA-B7.

NOTE: *The maximum and minimum occurrence depths are listed in Table 3-1. In general, this flow varies in thickness between 15 and 25 ft. Solid black circles represent where boreholes penetrate deep enough to encounter this unit, but no correlation was found in the appropriate depth interval. Open black circles represent where boreholes encountered the top of Unit TRA-B7 but did not penetrate to the bottom of the unit. Solid blue circles with black rims represent locations where boreholes penetrated through the TRA-B7 flow group.*

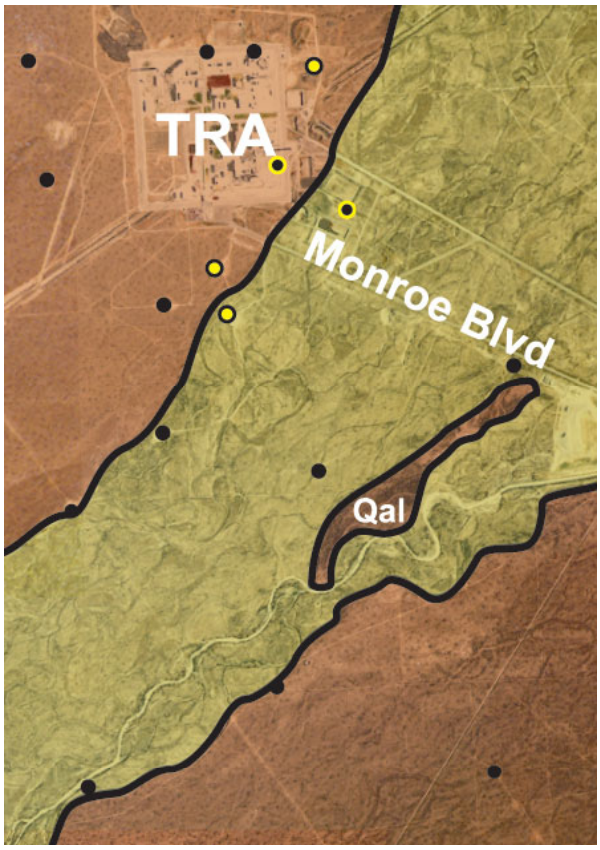

n. The subsurface extent of the intertrappean layer between Basalt Units TRA-B7 and TRA-B8.

NOTE: *Solid black circles represent where boreholes are deep enough to penetrate intertrappean material between these two basalt units, but intertrappean material and one or both basalts are absent from the stratigraphic column. Solid black circles with yellow rims represent where basalts TRA-B7 and TRA-B8 are both present in a borehole but no intertrappean material was logged between them. Yellow circles with black rims represent where intertrappean material was logged in the interval between the two basalt units.*

Figure 4-3. (continued).

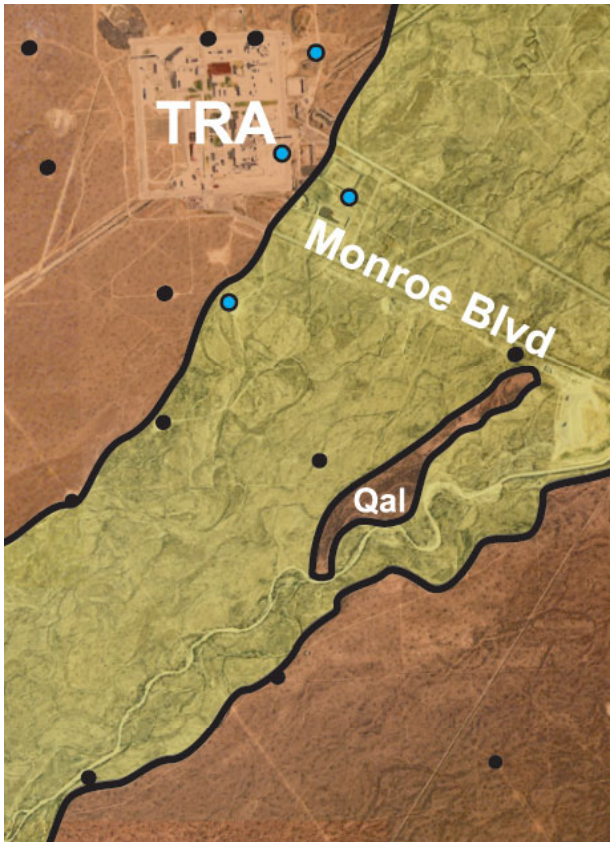

o. The subsurface extent of Basalt Unit TRA-B8.

NOTE: *The maximum and minimum occurrence depths are listed in Table 3-1. In general, this flow varies in thickness between 20 and 50 ft. Solid black circles represent where boreholes penetrate deep enough to encounter this unit, but no correlation was found in the appropriate depth interval. Open black circles represent where boreholes encountered the top of Unit TRA-B8 but did not penetrate to the bottom of the unit. Solid blue circles with black rims represent locations where boreholes penetrated through the TRA-B8 flow group.*

Figure 4-3. (continued).

4.4 Stratigraphic Correlation of the Test Reactor Area, Idaho Nuclear Technology and Engineering Center, and Naval Reactors Facility

Having placed the stratigraphy of Middle-1823 within the context of the TRA well field and with respect to CFA as represented by the VZRP, it is now necessary to investigate correlations to the east and north. Cross section M-M' (Figure A-14) is a transect from USGS-79 (at the southwest corner of TRA) to NPR-WO-2 east of INTEC. The stratigraphy on the TRA side of the cross section should be familiar. Basalt TRA-B5 pinches out to the east as TRA-B1 and -B2 pinch out to the west. Note that the USGS I-Flow locations in the TRA well field are below strata dated older than 786 ka.

The INTEC side of the cross section has several features of note, the most obvious of which are the general deepening of units to the east and a lack of correlations between TRA and INTEC. The best evidence for this are the depths of age dates under both facilities. A basalt in USGS-43 (shaded light blue,

Figure A-14) with an assumed age date of 350 ka based on correlations between Wells USGS-43 and WO-2, does not correspond to any known basalt in USGS-66. Basalt TRA-B1 in USGS-66 is assumed to have an age date of 414 ka, based on correlations with USGS-80. The shallowest basalt in USGS-43 that might be close to this date is a red basalt sequence at ~4,650 ft MSL (shaded light yellow-green on cross section M-M'), with an assumed age of 441 ka, based on a possible correlation with WO-2. This is a discrepancy in elevation of 200 ft between USGS-66 and USGS-43 if this unit is the same on both sides of Lincoln Boulevard. The basalt at 4,390 ft MSL in USGS-43 is thought to correlate to a basalt dated at 641 ± 54 ka in WO-2. Basalt TRA-B6 with an age of 643 ka in USGS-80 is at ~4,710 ft MSL. If TRA-B6 is the same as the 641 ka basalt in USGS-43, then there is a 400-ft vertical discrepancy between them. Note, however, that while the USGS I-Flow location in USGS-66 is 150 ft too deep, the USGS I-Flow depths on the INTEC side of the cross section correspond consistently with the 641 ka basalt of WO-2.

It is unlikely that the basalts of similar age, which are found on both the TRA and INTEC sides of Lincoln Boulevard, are actually the same units. If the basalts of similar age in USGS-66 and USGS-43 are the same, then their geochemistry should be very close if not nearly identical. Assuming that these basalts correlate to units of similar age in USGS-80 and WO-2, respectively, then we can compare the geochemical results from the appropriate depths in these wells. When we do so, however, we find that the concentrations of Ca, Fe, K, Mg, Na, Si and Ti are significantly different for basalt TRA-B3 in USGS-80, when compared to the 441 ka basalt at 4,581 ft MSL in WO-2. In addition, the TRA-B6 basalt in USGS-80 is significantly different in elemental concentrations of Ti, Fe, Mg, Ca, K and Na when compared to the 641 ka basalt at 4,304 ft MSL in WO-2.

Cross section N-N' (Figure A-15) is a transect from Middle-1823 to WO-2. This cross section is similar to M-M' (Figure A-14) in that the TRA side of the section does not correlate with the INTEC side. The gap between the two sides occurs between USGS-84 and USGS-39. The two tentative correlations of NGR peaks with sediments and cinders between USGS-84 and USGS-39 are based on NGR shape-matching alone, and should serve as a precautionary example of why relying on this method for correlation in the absence of other data types is the least preferred of correlation techniques available. If the age dates that we can infer for TRA-B3 and the 441 ka basalt at 4,600 ft MSL in USGS-39 are correct, then the tentative correlations between these two wells cannot exist as shown. The vertical discrepancy between the assumed 441 ka basalt in USGS-39 and TRA-B3 in USGS-84 is 200 ft. Given the information currently available, we cannot compare basalts with ages similar to AEC Butte on this cross section since we cannot identify one on the TRA side. We possibly could force a correlation based on cross section K-K' (Figure A-12). Such a correlation could equate the grey basalt at 4,670 to 4,650 ft MSL in Middle-1823 to TRA-B7. A basalt this old is deeper than the bottoms of the wells west of WO-2 on the INTEC side of the N-N' cross section. The basalt of similar age in WO-2 is at ~4,150 ft MSL. Examining the geochemical signatures of the 786 ka basalt from borehole TRA-5A and the basalt sample at 4,144 ft MSL in WO-2 shows the differences in concentrations for Ti, Fe, Mg, Ca, and K are the largest yet in this study for this kind of geochemical comparison.

While it is clear that we cannot correlate basalt units younger than ~780 ka between TRA and INTEC across the gap of the Big Lost flood plain, we can potentially correlate the deep sediment sequence between 3,865 and 3,350 ft MSL in Middle-1823 with the sediment sequence between ~3,220 and 2,670 ft MSL in WO-2. Significantly, this sequence in WO-2 is the sediment package identified as the 1.77–1.95 Ma playa-to-lacustrine “Olduvai Lake” sequence in 2-2A by Bestland et al. (2002) and correlated to WO-2 by Blair (2002). The correlation of these sediments between Middle-1823 and WO-2 depends on only NGR shape matching for now. This means there might be uncertainty as to the exact upper and lower bound of this sequence in Middle-1823 until more data is developed. Middle-1823 cores have been sampled for paleomagnetic analyses by the USGS, but the preliminary results are not yet reviewed or available. The pattern of normal and reverse polarity intervals determined by these preliminary data, however, suggests that the top of the sediment sequence that starts at 3,865 ft MSL

might belong to the Jaramillo and not the Olduvai Subchronozone (Anderson 2004[i]). The implications of these data are discussed in greater detail later in this text.

Cross section O-O' (Figure A-16) is a transect from USGS-123 at the southwest corner of INTEC to NRF-7 north of the NFR complex proper (see Figure 4-4). It is the longest and the most speculative of the cross sections. The first notable feature is the correlation gap between USGS-121 and the USGS-123/USGS-43/CCP-2 well group above ~4,550 ft MSL, and the correlation of the sequence roughly equivalent to the USGS I-Flow in USGS-121, USGS-43, and USGS-123 below. The INTEC I-Flow sequence likely is present at the appropriate depths in CPP-2, but we cannot identify it with any confidence using NGR shape matching, which is the only correlation method available for this well at this time. The CPP-2 lithology is not sufficiently detailed and the NGR log lacks the marker beds that would enable the INTEC I-Flow correlation with the other three INTEC wells in this cross section.

This pattern of "deep correlations below 400 ft bls but no correlations above 400 ft bls" is also seen in the geochemical profiles for USGS-121 and USGS-123 (Figure 4-5), a result described in detail by Reed, Bartholomay, and Hughes (1997). In this figure, it is obvious that the geochemical trends above 4,550 ft MSL do not match, while the trends below 4,550 ft MSL have a high degree of correlation. The anomalous Al peak in USGS-121 at 4,385 ft MSL is not present at the equivalent position at ~4,400 ft MSL in USGS-123, but this could be the consequence that there are four sample analyses in this interval in USGS-121 as compared to the two samples in USGS-123. This is another example of different geochemical sampling densities potentially degrading the quality of the geochemical profiling. It would be valuable to resample this interval in USGS-123 to see if this Al spike exists on the southern boundary of the INTEC area as well as the northern boundary.

It is apparent that we cannot correlate between the NRF area and INTEC. The correlation gap coincides with the location of the Fire Station Well (FSW). Like TRA-2, this well also lacks geophysical logs. The lithology shown on the cross section is from the lithological log of this well as compiled by S. Ansley (who also compiled the lithology for TRA-2 and TRA-4 for this study). The thinly bedded basalt and sediment sequence between 4,470 and 4,430 ft MSL in FSW is possibly the same as a similar sequence starting at 4,470 ft MSL in USGS-98, but these sequences cannot be correlated with certainty without additional data. Relying on old lithological logs alone for two wells a mile apart is not considered a defensible basis for a correlation. If geophysical logs were available for FSW, a correlation between the sequence starting at 4,470 ft MSL could exist in these two wells.

The correlations from INEL-1 north to NRF seem to be less subject to the interfingering effect seen in units closer to the flood plain in the TRA/INTEC region of the Site. It is not unreasonable that this greater continuity in the subsurface NRF might extend as far south as FSW. The stratigraphy for NRF is modified from Champion et al. (2002). The locations of the coreholes that Champion et al. (2002) cite (i.e., NA-89-04, NA-89-05, and B18-1) are all ~200 ft from wells NRF-1, NRF-2, and NRF-8. The red circles on Figure 4-4 show the locations of the wells, while the yellow circles with red rims show the coreholes paired with them. Unlike other areas considered in this study, the stratigraphy for NRF (Cross Section O-O', Figure A-16) is based on core logs, age dates, and paleomagnetic inclinations, but not on geophysical logs.

---

i. Anderson, S. R., USGS, personal communication to C. Helm-Clark, INL, February 19, 2004.

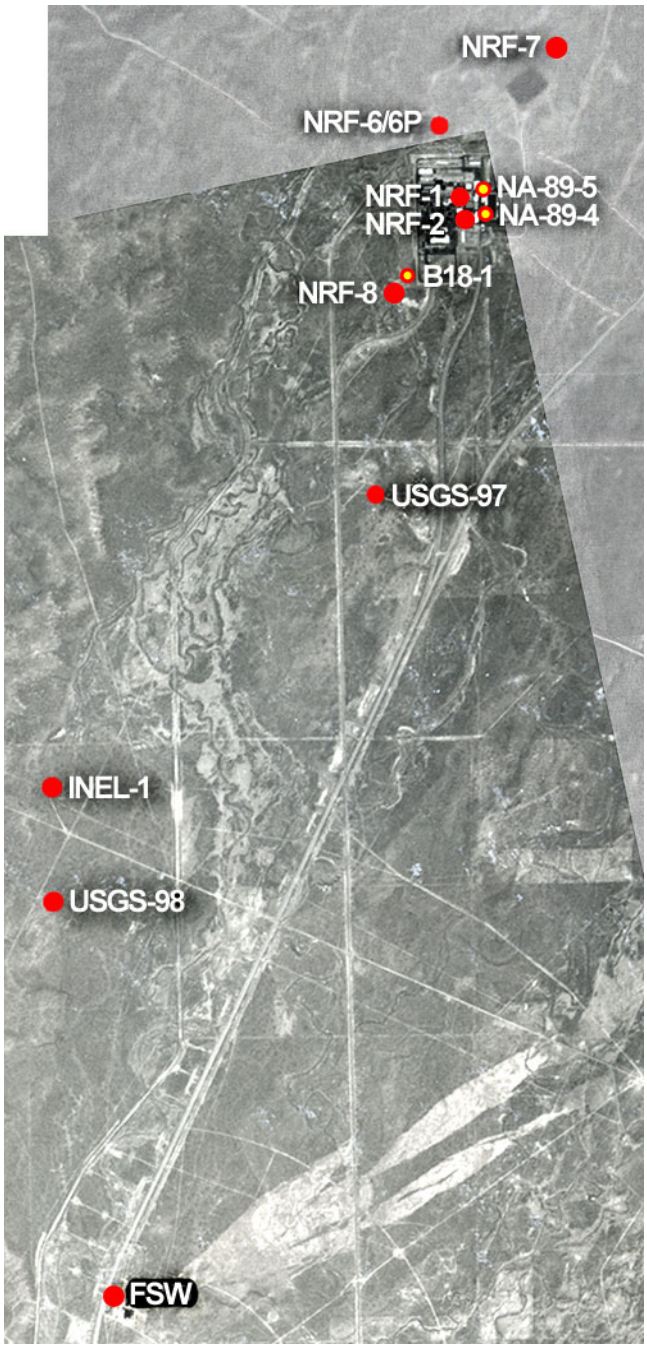

Figure 4-4. Map showing the wells in or near the Naval Reactors Facility that were analyzed for this study.

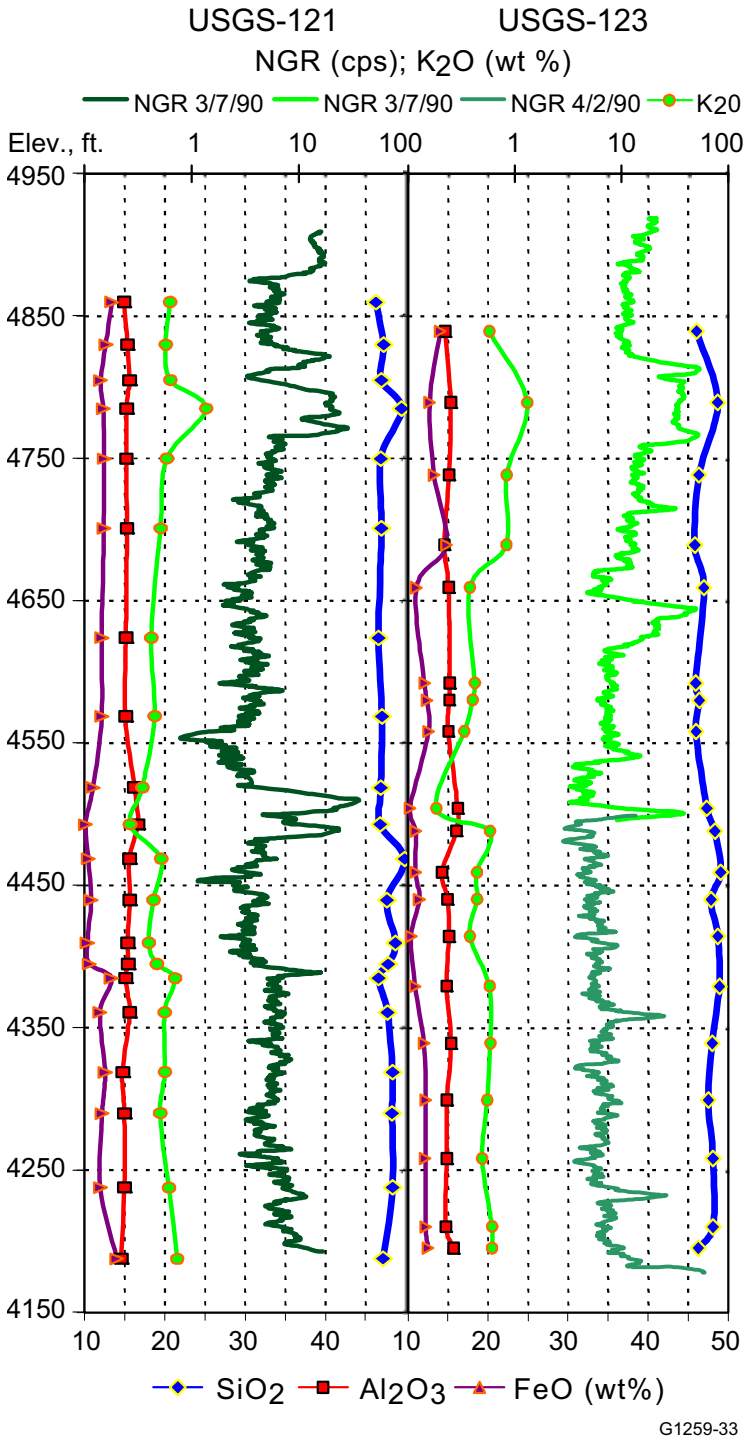

Figure 4-5. Geochemical profiles for the major elements as oxides for Wells USGS-121 and USGS-123.

NOTE: *The NGR logs are also shown, since the comparison of the K profiles (see Table 4-4) and the NGR logs indicate that the NGR logs do not depend on K alone here (cf., Anderson and Bartholomay 1995).*

Table 4-4. Major element geochemical data for Wells USGS-121 and USGS-123.

Well	Elev., ft	Depth, ft	Depth, m	SiO2	TiO2	Al2O3	FeO*	MgO	CaO	Na2O	K2O
USGS-121											
	4860	50	15.2	46.2	2.74	15.0	13.4	8.36	10.29	2.63	0.63
	4830	80	24.4	47.2	2.54	15.4	12.7	7.97	10.29	2.65	0.58
	4805	105	32.0	46.9	2.15	15.6	12.1	9.16	10.34	2.54	0.64
	4785	125	38.1	49.4	2.62	15.3	12.4	6.06	9.29	2.83	1.36
	4750	160	48.8	46.8	2.30	15.2	12.5	9.05	10.39	2.40	0.59
	4701	209	63.7	46.9	2.29	15.3	12.5	8.40	10.97	2.44	0.51
	4624	286	87.2	46.5	1.93	15.2	12.2	9.86	10.87	2.32	0.42
	4569	341	103.9	47.0	2.09	15.1	12.2	9.43	10.69	2.32	0.45
	4519	391	119.2	46.9	1.53	16.3	11.1	9.17	11.76	2.48	0.35
	4493	417	127.1	46.7	1.17	16.7	10.2	10.27	12.19	2.16	0.27
	4469	441	134.4	49.8	1.76	15.6	10.5	7.82	10.82	2.55	0.52
	4440	470	143.3	47.6	1.51	15.7	10.9	10.46	10.79	2.18	0.44
	4410	500	152.4	48.7	1.41	15.4	10.4	10.01	10.85	2.41	0.40
	4395	515	157.0	47.8	1.42	15.5	10.7	10.65	10.88	2.22	0.47
	4385	525	160.0	46.6	2.82	15.1	13.4	7.21	10.88	2.56	0.70
	4361	549	167.3	47.7	2.23	15.7	12.0	7.68	10.83	2.72	0.56
	4319	591	180.1	48.3	2.41	14.8	12.7	7.53	10.49	2.57	0.56
	4290	620	189.0	48.2	2.25	15.0	12.3	8.33	10.31	2.44	0.51
	4238	672	204.8	48.3	2.27	15.0	12.0	8.02	10.41	2.62	0.61
	4188	722	220.1	47.1	3.07	14.6	14.0	6.84	9.81	2.76	0.73
	Original Source: Reed, Bartholomay, and Hughes (1997).										
USGS-123											
	4839	80	24.4	46.1	3.04	14.6	14.0	8.01	10.10	2.76	0.58
	4789	130	39.6	48.7	2.70	15.3	12.7	6.23	9.41	2.83	1.30
	4738	181	55.2	46.3	2.63	15.1	13.3	8.11	10.19	2.64	0.84
	4689	230	70.1	45.8	3.14	14.5	14.8	7.92	9.54	2.55	0.83
	4659	260	79.2	47.0	1.61	15.1	11.0	11.16	11.19	2.14	0.38
	4592	327	99.7	45.9	1.73	15.2	12.1	10.87	10.94	2.24	0.42
	4580	339	103.3	46.4	2.00	15.2	12.3	9.83	10.89	2.31	0.40
	4558	361	110.0	46.0	2.05	15.0	12.6	9.87	11.05	2.42	0.34
	4504	415	126.5	47.3	1.16	16.2	10.2	10.18	12.16	2.21	0.18
	4488	431	131.4	48.3	1.87	16.1	11.0	8.22	11.02	2.46	0.59
	4459	460	140.2	49.1	1.79	14.2	11.0	9.14	11.05	2.53	0.44
	4440	479	146.0	47.8	1.80	14.9	11.4	10.08	10.65	2.33	0.44
	4414	505	153.9	48.7	1.38	15.1	10.4	10.18	10.91	2.29	0.38
	4379	540	164.6	48.9	1.70	14.8	10.9	9.73	10.39	2.40	0.58
	4339	580	176.8	48.0	2.30	15.4	12.0	7.63	10.76	2.60	0.59
	4299	620	189.0	47.5	2.24	14.9	12.2	8.46	10.79	2.63	0.55
	4258	661	201.5	48.1	2.14	14.8	12.2	8.74	10.23	2.61	0.49
	4210	709	216.1	48.1	2.32	14.7	12.2	8.24	10.28	2.74	0.61
	4195	724	220.7	46.3	2.19	15.7	12.5	9.22	10.47	2.39	0.61
	Original Source: Reed, Bartholomay, and Hughes (1997).										

4.5 Plio-Pleistocene Paths of the Big Lost River and Their Effect on Deep Correlations

Blair and Link (2000), Blair (2002), and Bestland et al. (2002) have concluded that the northeast drainage of the Big Lost River between the AVH and the Big Lost Range is approximately 2 Ma, based on the presence of widespread lacustrine rocks deep in the subsurface under the current flood plain. The age of these sediments is based on their occurrence in Wells WO-2 and 2-2A, where normal paleomagnetic inclinations and a K/Ar date of 1.86 Ma places these beds firmly in the Olduvai Normal Polarity Subchron—hence the origin of the common-use name for these sediments as the "Olduvai Lake" or "Olduvai Lake Beds."

The Olduvai Lake sediments have been identified as far north as Well TCH-1 at TAN. Well TCH-1 is located north of the sinks of both the Big Lost and Little Lost Rivers and south of the sinks of Birch Creek. Given the current geography of the drainages out of the Northern Rockies onto the ESRP, it is a pertinent question whether the Olduvai beds actually have Big Lost River and Little Lost River components. The modern sinks receive sediments from all three INL watersheds, and if the AVH existed or was rising at ~2 Ma, then the paleo-sinks that formed the Olduvai Lake Beds also would have received this mix of sediments.

Blair (2002) identified Olduvai Lake sediments in Well C1A at the RWMC. This correlation is called into question, however, by a new age date for C1A basalt at 1,195 ft bls (Helm-Clark and Rodgers 2004). This $^{40}Ar/^{39}Ar$ date of 0.82 ± 0.16 Ma suggests these sediments are much younger than the Olduvai Subchron. If the new Helm-Clark and Rodgers (2004) age date is correct, then Blair's (2002) identification of C1A Olduvai sediments might be too old. Before proceeding further on the subject of deep correlations, it is germane to examine where the path of the Big Lost River might have been in the past.

The paleo-paths of the Big Lost River will exert a first-order effect on possible deep correlations. If the river was indeed flowing northeastward during the Early Pleistocene, then continuity and coherency of deep deltaic and fluvial sediments could indeed exist under the entire length of the flood plain from RWMC to TAN. If the paleo-paths of the Big Lost River pointed in some other direction, such as south across the plain toward the ancestral Snake River, then some of the deep sediment packages at the Site might not be correlable. The movement and deposition of gravel-sized sediment on a flood plain occurs by bedload transport in river and stream waters traveling faster than 10 cm/sec, a velocity that is only achieved on a flood plain in the high-energy environment of a flood event (Graf 1971). Though sandy sediments are much more common in the fluvial environment, sands can be found in other depositional settings, whereas gravels can only be moved on a plain by flood waters. A gravel, therefore, is the unmistakable signature of a river at flood.

A survey of subsurface gravels for the TRA well field and environs is summarized in Table 4-5. Subsurface gravels are not uncommon under the flood plain above 4,500 ft MSL throughout the study area. In wells that penetrate below 4,500 ft MSL, however, deep gravels are not encountered under NRF; INTEC, and the old fire station site north of INTEC; the southern half of the TRA well field; and the VZRP. Deep gravels just above and below 4,200 ft MSL were encountered at the New Production Reactor (NPR) site and directly under the TRA. Very few wells penetrate deeper than 4,200 ft MSL. They include: TRA-5, INEL-1, WO-2 and 2-2A. Of these, only TRA-5 and 2-2A encountered logged gravel below 4,000 ft MSL. The distribution of gravel older than ~780 ka in the subsurface suggests the flood

Table 4-5. Depths of subsurface gravels.

A Partial List of Interbeds Containing Gravels at INTEC, TRA, and NRF and Their Environs								Wells with No Gravels Mentioned in Lithological Logs	
Well Name	Nearest Facility	Gravel Logged in Interbed TRA-I3	Gravel Logged in Interbed TRA-I4	The Gravel Unit Above TRA-B6 and Below TRA-I5	Gravels below Basalt TRA-B7	INTEC Gravels between Basalts Dated at 441ka and 491ka	Gravels Not Associated With Any Named and/or Dated Units	Well Name	Nearest Facility
Middle-1823	CFA			4,710			4,850		
USGS-39	CFA					4,540	4,435		
								ICPP-SCI-V-213	CFA
USGS-43	INTEC					4,540		ICPP-SCI-V-214	CFA
USGS-47	INTEC						4,590	MTR-Test	TRA
USGS-49	INTEC						4,770	TRA-5A/PZ1	TRA
USGS-51	INTEC					4,530		TRA-6A	TRA
USGS-57	INTEC					4,530		TRA-7	TRA
USGS-59	INTEC					4,530	4,660, 4,620	USGS-53	TRA
								USGS-54	TRA
WO-2	NPR						4,190, 4,028	USGS-55	TRA
								USGS-56	TRA
INEL-1	NRF						4,350, 4,340	USGS-60	TRA
USGS-97	NRF						4,740	USGS-61	TRA
								USGS-62	TRA
2-2A	TAN						3,927, 2,951	USGS-63	TRA
								USGS-65	TRA
Site-19	TRA		4,770					USGS-68	TRA
TRA-2	TRA				4,180, 4160		4,350, 4,230, 4,210	USGS-69	TRA
TRA-4	TRA				4,180, 4170			USGS-70	TRA
TRA-5 (Disp.)	TRA			4,710			3,710	USGS-71	TRA
TRA-8	TRA						4,690	USGS-73	TRA
USGS-58	TRA			4,740				USGS-78	TRA
USGS-64	TRA			4,760				USGS-79	TRA
USGS-66	TRA			4,750			4,590	USGS-82	NPR
USGS-72	TRA	4,780						USGS-84	CFA
USGS-74	TRA		4,750					USGS-98	NRF
USGS-76	TRA			4,710				USGS-121	INTEC
USGS-80	TRA			4,760				USGS-123	INTEC

CFA = Central Facilities Area
INTEC = Idaho Nuclear Technology and Engineering Center
NPR = New Production Reactor
TAN = Test Area North
TRA = Test Reactor Area

plain of the Big Lost River might have been shifted eastward away from the mountains, based on the existence of deep gravels under TRA but not under INTEC. To ascertain the possibility of paleo-channels of the Big Lost River outside of the Big Lost Trough would entail an examination of well logs south and east of the Site (Thackery 2003[j]) and is outside the current scope of work.

4.6 Correlation of Deep Sediments in Middle-1823 and Other Deep Wells

Correlations below ~4,000 ft MSL are difficult because very few boreholes penetrate this deep. This lack of deep wells results in a lack of geochronological data at depth. Geochemical profiling has been helpful for the few boreholes that have been analyzed (e.g., Reed, Bartholomay, and Hughes 1997; Hughes, McCurry, and Geist 2002), but for the deep holes considered here (see Figure 4-6), these data exist only for two wells: WO-2 and 2-2A. In the absence of other data types, correlations must rely on shape matching the geophysical logs. The most useful log for shape matching is the NGR log but only if there are flows and interbeds that can act as marker beds. Fortunately, such marker beds exist in TRA-5 and Middle-1823, starting at elevations of 3,910 and 3,865 ft MSL, respectively. The pattern of the NGR log for these interbeds and basalts closely resembles that seen in WO-2 at 3,260 ft MSL. Based on the similarity of the NGR logs for these intervals, the WO-2 strata between 3,260 and 3,130 ft MSL could be the same as those from 3,780 to 3,910 ft MSL in TRA-5 and from 3,685 to 3,865 ft MSL in Middle-1823. This interval in WO-2 includes a basalt with an age date of 1.856 ± 0.024 Ma (Anderson, Liszewski, and Cecil 1997) during the Olduvai Normal Polarity Subchron. If the correlation of these three intervals is correct, we can then identify these deep sediments in Middle-1823 and TRA-5 as part of the Olduvai Lake complex, as described by Bestland et al. (2002).

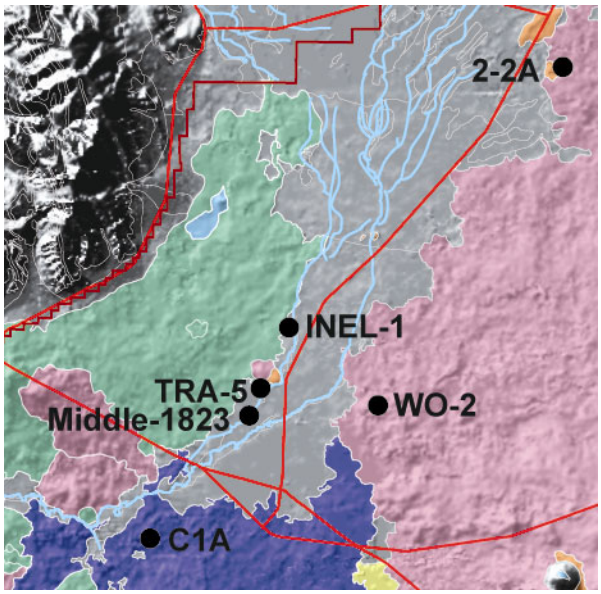

Figure 4-6. Map of wells with possible Olduvai Subchron Lake sediments.

Below the sediments from 3,780 to 3,910 ft MSL in TRA-5 and from 3,685 to 3,865 ft MSL in Middle-1823 are deep sequences of sediments in various states of lithifaction. A similar sequence of basalt-intercalated, variably lithified sediments is also present in INEL-1. It is not clear whether these sediment layers can be correlated from TRA-5 and Middle-1823 to INEL-1 on the basis of NGR shape

j. Thackery, G., ISU, personal communication to C. Helm-Clark, INL, October 2003.

matching alone, nor is it certain that any of the thick sediments in these three wells correlate with the only significant deep package of sediments in WO-2 (i.e., known Olduvai Lake beds). It is worth noting that a very thick package of deep sediments occurs from 3,400 to 3,950 ft MSL in Well USGS-15, midway between NRF and Howe Point. If we include the thick sediments at depth in Wells 2-2A and TCH-1, then it can be safely said that thick sequences of sedimentary materials seem to be a feature of deeply penetrating wells under the modern Big Lost Trough. Unfortunately, comparing the deep sediments from Middle-1823, TRA-5, and INEL-1 with those in USGS-15 is not possible since there are no geophysical logs for USGS-15 deeper than ~600 ft bls, and the available lithologic logs are not sufficiently detailed for meaningful comparisons.

Bestland et al. (2002) described the lacustrine sediments of the Olduvai Lake complex from Well-2-2A. They noted that these sediments were of normal magnetic polarity, as would be expected of materials deposited during the Olduvai Subchron. While the Olduvai sediments in Wells 2-2A and WO-2 can be correlated by core petrology, geochemical profiling, age, and magnetic polarity, none of these data types are available for INEL-1. We have tentatively identified the Olduvai Lake sediments in this well by shape matching the Olduvai Lake and basalts 400 ft above it with the same interval in Well 2-2A. The closed-transect fence diagram shown on Figure A-17 illustrates what these correlations would look like if these deep sediment intervals all belong to the Olduvai Subchronozone.

The postulated subsurface depression of the Big Lost Trough is essentially a shallow bathtub shape whose long axis is subparallel with the path of the Big Lost River from RWMC toward TAN. The short axis is perpendicular to the path of the river on the Site. The western, eastern, and southern lips of the trough are assumed to border the BLR, the AVH, and the AVH/Arco Rift intersection by Big Southern Butte, respectively. The fence diagrams B-B', C-C', and D-D'-D" in Anderson and Liszewski (1997) convey the general sense of this shallow bathtub shape whose bottom is taken as the base of the regional aquifer. South of the AVH and Arco Rift, the bottom of the aquifer and the general dip of strata is assumed to dip southward into the plain (Anderson and Liszewski 1997). The fence diagram in Figure A-17 is consistent with this model of the Big Lost Trough where the changing dip of the Brunhes-Matuyama transition and Olduvai Beds along the C1A/WO-2/2-2A Transect reflect the shallow bathtub shape. It is important to note that the generalized bathtub character of the trough hinges on the shallowing of flows and beds from the center of the Site toward RWMC.

Studies by Anderson and Liszewski (1997), Blair and Link (2000), Blair (2002), and Bestland et al. (2002), among others, detail the pervasive lacustrine nature of the Olduvai Lake sediments. The implication of these collective interpretations is that these sediments were deposited at the same elevation in a deltaic to lacustrine environment. If this is true, then there has been major relative subsidence in the center of the Site since ~1.8 Ma because no other means exists to create the 800-ft vertical discrepancy of the postulated Olduvai beds between Wells INEL-1 and WO-2, the 650-ft vertical discrepancy of the postulated Olduvai beds between Wells TRA-5 and WO-2, or the 400-ft discrepancy of the postulated Olduvai beds between Wells C1A and WO-2.

4.7 Problems with the Subsurficial Big Lost Trough Introduced by New Age Dates

Helm-Clark and Rodgers (2004) have obtained new age dates for two subsurface basalt cores collected at 340 ft bls from Well 2-2A, and at 1,195 ft bls from Well C1A. An additional sample was collected at 583 ft bls from Well C1A, but dating this sample did not succeed. The sample from Well CH-2-2A collected at 340 ft bls (103.6 m) yielded a plateau age of 0.71 ± 0.06 Ma on a groundmass concentrate from a reverse-polarity basalt flow (depth 97-120 m, inclination = -74.9 [Bestland et al. 2002]). The sample from Well C1A from a depth of 1,195 ft bls (364.2 m) yielded a plateau age of

0.82 ± 0.16 Ma on a groundmass concentrate of a normal-polarity basalt flow. The age spectra for the CH-2-2A sample was flat, and for the C1A sample, it was very slightly discordant.

In CH-2-2A, a negative polarity (inclination = -73.9 [Bestland et al. 2002]) basalt flow at a depth of 90.9 m was dated at 0.58 ± 0.15 Ma using $^{40}Ar/^{39}Ar$ by Hughes, McCurry, and Geist (2002). There are several acceptable explanations for these two CH-2-2A dates in reverse-polarity basalt. The first is that the Hughes, McCurry, and Geist (2002) date and the Helm-Clark and Rodgers date (2004) are both too young (i.e., that both dates are slightly in error). This view of the new 2-2A dates is potentially bolstered by the fact that the two flow units where the samples were collected have almost identical paleomagnetic inclinations. Another viable explanation is that the later date could belong to the Big Lost Subchron of Champion, Lanphere, and Kuntz (1988) and the former to the very top of the Matuyama Chronozone.

The new age date for C1A is more problematic. The C1A reverse-polarity intervals are at depths of 121–173 m, 213–326 m, and below ~449 m (Champion et al. 2002). If the C1A age date at 364.2 m depth is correct, then the normal polarity basalts from 362–425 m cannot belong to the Olduvai Subchron as previously thought (e.g., Blair 2002), but belong either to an unidentified paleomagnetic excursion, the younger Jaramillo Subchron, or at the bottom of the Bruhnes Chronozone at ~780 ka. The C1A sediment interval at ~425–449 m, which has previously helped to define the shallowing lip of the Big Lost Trough (Blair 2002) based on the assumption that these sediments belong to the Olduvai Subchronozone, might actually be younger than this. If this new C1A date is correct, then the Olduvai could be much deeper than the sediments identified by Blair (2002) as the Olduvai Lake Beds.

Figure A-18 shows a fence diagram transect from C1A to 2-2A through wells on the east side of the flood plain, assuming that the C1A reverse-polarity basalts dated by Helm-Clark and Rodgers (2004) belong to the Jaramillo Subchronozone. While there is no identified Jaramillo interval in WO-2, the Jaramillo has been identified in Well 2-2A. Using the Bruhnes-Matuyama polarity transition between 2-2A and WO-2, and the postulated position of the Jaramillo in 2-2A and C1A, the dip of the deep strata on the Site no longer shallow upwards toward RWMC, but instead plunge downward to the southwest.

4.8 Problems with the Subsurficial Big Lost Trough Introduced by New Paleomagnetic Data

Preliminary paleomagnetic analyses of the Middle-1823 core (Anderson 2004 [see footnote h]) suggest that the Middle-1823 sediment layers starting at 3,865 ft MSL might belong to the Jaramillo Normal Polarity Subchron (0.98 – 1.05 Ma) since they are intercalated with normal polarity basalts underneath higher-elevation reverse polarity basalts from ~4,200 to ~4,000 ft MSL. If the polarities from the preliminary paleomagnetic results are shown on the stratigraphic column for Middle-1823 and compared to C1A and TRA-5, the sequence of sediment layers, normal polarity basalts, and reverse polarity basalts appears to be similar for C1A, Middle-1823, and TRA-5 (see Figure A-19). The new C1A age date, the paleomagnetic data for C1A, and the preliminary paleomagnetic data for Middle-1823 are complimentary datasets. If both the age date and the new inclination data are confirmed, then this is defensible evidence that the deep sediment sequences starting at 3,640 ft MSL in Well C1A, 3,865 ft MSL in Middle-1823, and 3,910 ft MSL in TRA-5 belong to the Jaramillo Subchronozone and not to the Olduvai Lake.

If the deep sediment package starting at 4,065 ft MSL in INEL-1 is the Olduvai Lake Bed, but the sediments from 3,780 to 3,910 ft MSL in TRA-5 and from 3,685 to 3,865 ft MSL in Middle-1823 belong to the younger Jaramillo, then this could provide concrete evidence that northwest trending lines of volcanic vents, like that through AEC Butte, form localized rift zones across which strata cannot be correlated. This supports a scenario of time-pervasive volcanic rift features that have disrupted the

continuity of horizontal flows and sediments across the Site during the Quaternary and might exert some form of northwest-southeast control on the generally northeast-to-southwest flow of groundwater in the regional aquifer, as suggested by Anderson, Kuntz, and Davis (1999).

4.9 The Geochemistry of Pre-Olduvai Basalts

Major and trace element concentrations for Wells 2-2A, WO-2, and C1A are tabulated in Tables 4-6 through 4-11 and shown in Figures 4-7 and 4-8, respectively. Values for major elements are reported as weight percent of their oxides, and values for trace elements are reported as parts per million. Data for this analysis is from the December 2002 version of the Idaho State University ESRP geochemical database maintained by Profs. Scott Hughes and Michael McCurry.

The geochemical signature of the basalts immediately below the Olduvai Lake sediments is characterized by higher iron values (>14%) in comparison with aluminum (<14%), and higher titanium values (~3%) in comparison to sodium (~2.5%) (Figure 4-7). The titanium and the iron values (measured as oxides) are both near the maximum possible values for these two elements in ESRP basalts. Normally, the values for aluminum are higher than those for iron, so the flip in these numbers in the basalts immediately below the Olduvai sediments is distinctive. Values for silica (ranging 46%–50%) in the basalts immediately below the Olduvai Lake are at a local minimum, less than 47% (not shown on Figure 4-7). Trends in trace element concentrations for these pre-Olduvai basalts are at local maximum in Zn (140-160 ppm), with rising values of Sr (290-310 ppm) sloping toward a local maximum 100 ft below the base of the Olduvai (320-350 ppm), and average values for nickel (70-100 ppm).

The limitations of using discrete-sample geochemical data are apparent here. The sampling density of these analyses was not driven by the needs of stratigraphic correlation, but by the goal of examining trends in the geochemical evolution of ESRP basalts through time. This practice has led to sampling density that is occasionally sparse in intervals we would like to compare (e.g., at 1,750–1,850 ft bls in WO-2). In addition, because of the nonuniformity of sample spacing and low sampling density in places, we cannot be sure that local minimum and maximum geochemistry values are accurately represented by the current dataset. We also are not knowledgeable about the effects of low-temperature alterations on geochemical compositions, since no one to date has performed a comprehensive study of this in ESRP basalts. The results of Scarberry's research (2003) on the geochemistry of the RWMC F-flow certainly indicate that this is an important problem that needs to be addressed before the potential of geochemical analyses for stratigraphic correlation can be exploited fully.

The geochemical data available for C1A is extremely sparse below 600 ft bls, which is unfortunate in terms of using geochemistry for correlations in the southern portions of INL. Blair (2002) and Champion et al. (2002) have placed the Olduvai Lake sediments at 1,400 to 1,450 ft bls in C1A on the basis of paleomagnetic inclinations since these sediments and the basalts immediately above them fall into the third interval of normal polarity in this well. In other deep wells, such as 2-2A and WO-2, the third interval of normal polarity has been dated at ~1.856 Ma. It is not unreasonable, therefore, to assign an Olduvai age to the third normal polarity interval in C1A in the absence of other data. The new C1A age date (Helm-Clark and Rodgers 2004), however, strongly suggests that this normal polarity interval is the base of the Brunhes or the top of the Jaramillo. If the new date is correct, then the sediments at 1,400–1,450 ft bls likely are not the Olduvai Lake interval, but are actually much younger. This implies that the Olduvai sediments, if they exist at the C1A location, are deeper than previously thought and are too deep to intersect the current C1A corehole, as is shown on Figure A-18.

Table 4-6. Major element geochemical data for Well 2-2A.

Well	Elev. (ft)	Depth (ft)	Depth (m)	SiO2	TiO2	Al2O3	FeO*	MgO	CaO	Na2O	K2O
2-2A											
	4,885	45	13.7	46.9	2.72	14.9	14.1	7.67	9.69	2.61	0.62
	4,876	54	16.5	47.1	2.70	15.0	13.6	7.76	9.80	2.66	0.63
	4,664	266	81.1	45.7	2.89	14.3	14.5	8.45	10.09	2.55	0.50
	4,632	298	90.8	45.6	2.92	14.4	14.8	8.04	9.99	2.59	0.65
	4,597	333	101.5	45.7	3.09	14.2	14.6	7.70	10.50	2.52	0.59
	4,578	352	107.3	45.8	3.09	14.3	14.7	7.93	9.78	2.69	0.64
	4,537	393	119.8	47.0	2.28	15.7	12.6	8.23	10.87	2.56	0.20
	4,508	422	128.6	47.1	3.18	14.2	14.0	7.17	10.04	2.49	0.69
	4,487	443	135.0	46.5	3.24	14.1	15.5	7.04	9.55	2.46	0.59
	4,468	462	140.8	46.9	3.31	14.0	15.0	7.20	9.54	2.52	0.56
	4,448	482	146.9	48.4	2.57	15.2	13.4	6.69	9.29	2.72	0.75
	4,435	495	150.9	48.3	2.60	15.0	13.5	6.90	9.31	2.74	0.70
	4,417	513	156.4	47.8	2.69	14.9	14.1	7.03	9.21	2.64	0.79
	4,387	543	165.5	48.2	2.76	14.7	13.9	6.91	9.26	2.70	0.71
	4,344	586	178.6	47.9	2.40	15.2	13.6	7.55	9.28	2.75	0.54
	4,322	608	185.3	47.9	2.61	14.6	14.1	7.30	9.29	2.75	0.55
	4,312	618	188.4	48.0	2.56	14.8	13.8	7.45	9.34	2.80	0.48
	4,275	655	199.6	47.3	1.79	14.8	13.4	9.51	9.97	2.43	0.26
	4,264	666	203.0	47.3	1.78	14.7	13.3	9.71	9.99	2.49	0.31
	4,252	678	206.7	47.6	1.81	14.9	12.8	9.56	10.06	2.42	0.34
	4,213	717	218.5	47.6	1.85	14.8	12.7	9.69	9.95	2.42	0.37
	4,174	756	230.4	46.8	2.55	15.5	13.7	7.69	9.83	2.69	0.49
	4,160	770	234.7	46.8	2.47	15.7	13.6	7.85	9.80	2.70	0.42
	4,151	779	237.4	46.0	2.40	15.3	13.6	8.06	10.78	2.67	0.42
	4,122	808	246.3	46.5	2.44	15.5	13.5	8.16	9.95	2.76	0.40
	4,109	821	250.2	46.4	2.34	15.5	13.6	8.15	10.07	2.76	0.37
	4,087	843	256.9	46.6	2.37	15.3	13.7	8.14	9.85	2.76	0.45
	4,021	909	277.1	47.5	2.36	15.3	13.6	7.60	9.67	2.76	0.60
	4,000	930	283.5	47.6	2.42	15.1	13.6	7.70	9.69	2.60	0.71
	3,975	955	291.1	48.0	2.25	15.1	12.8	8.21	9.72	2.66	0.57
	3,760	1,170	356.6	47.6	3.29	14.0	14.9	6.63	9.63	2.52	0.54
	3,740	1,190	362.7	47.5	3.29	13.9	15.1	6.71	9.51	2.54	0.58
	3,718	1,212	369.4	46.9	3.46	13.8	15.7	6.71	9.65	2.58	0.42
	3,696	1,234	376.1	47.3	3.24	13.9	15.4	6.76	9.54	2.49	0.61
	3,688	1242	378.6	47.2	3.15	14.0	15.9	6.85	9.28	2.32	0.59
	3,661	1,269	386.8	48.1	2.97	14.4	13.6	7.31	9.57	2.50	0.72
	3,646	1,284	391.4	48.5	3.04	13.7	13.6	6.89	10.06	2.61	0.86
	3,628	1,302	396.8	47.7	2.90	14.5	13.6	7.30	9.66	2.70	0.82
	3,606	1,324	403.6	47.9	2.99	14.3	14.1	7.09	9.76	2.45	0.68
	3,595	1,335	406.9	48.4	3.00	14.5	13.2	6.95	9.69	2.64	0.77
	3,355	1,575	480.1	47.0	2.33	14.9	12.7	8.19	11.95	2.31	0.10

Table 4-6. (continued).

Well	Elev. (ft)	Depth (ft)	Depth (m)	SiO2	TiO2	Al2O3	FeO*	MgO	CaO	Na2O	K2O
2-2A											
	3,317	1,613	491.6	47.6	2.27	15.3	12.2	9.45	10.08	2.28	0.20
	3,153	1,777	541.6	47.9	2.30	16.3	13.5	7.16	9.50	2.59	0.27
	3,019	1,911	582.5	47.8	2.79	14.7	13.5	7.62	10.26	2.37	0.32
	3,003	1,927	587.3	47.7	2.81	14.4	13.8	8.43	9.95	2.12	0.14
	2,984	1,946	593.1	47.5	2.89	14.4	14.3	7.43	10.37	2.28	0.14
	2,946	1,984	604.7	47.7	2.37	14.9	12.9	8.14	10.90	2.20	0.25
	2,927	2,003	610.5	48.5	2.47	15.0	13.9	5.59	10.72	2.67	0.47
	2,907	2,023	616.6	48.0	2.47	14.6	13.8	6.50	10.28	2.81	0.76
	2,891	2,039	621.5	48.4	2.46	14.3	14.0	6.28	10.31	2.67	0.83
	2,854	2,076	632.8	47.3	2.36	15.1	13.8	7.60	10.35	2.51	0.38
	2,834	2,096	638.9	47.2	2.42	14.9	14.4	7.25	10.26	2.49	0.45
	2,790	2,140	652.3	47.2	2.36	15.4	13.8	7.62	10.05	2.54	0.45
	2,774	2,156	657.1	47.3	2.38	15.2	14.0	7.50	10.16	2.49	0.40
	2,729	2,201	670.9	47.5	1.97	16.1	12.8	7.99	10.27	2.43	0.34
	2,706	2,224	677.9	48.9	2.18	16.4	12.2	5.84	11.02	2.66	0.33
	2,661	2,269	691.6	47.4	2.17	15.6	13.1	8.13	10.25	2.41	0.31
	2,625	2,305	702.6	47.3	2.28	15.6	13.4	7.75	10.30	2.39	0.34
	2,603	2,327	709.3	47.4	2.25	15.4	13.2	7.12	10.97	2.59	0.36
	2,581	2,349	716.0	47.9	1.65	14.9	11.5	8.97	12.15	2.09	0.23
	2,576	2,354	717.5	47.8	1.63	14.8	11.7	8.95	12.26	2.13	0.23
	2,553	2,377	724.5	47.7	1.93	14.9	12.2	8.03	11.72	2.41	0.36
	2,538	2,392	729.1	48.3	2.44	14.6	13.5	6.61	10.93	2.51	0.46
	2,527	2,403	732.4	47.8	2.37	14.9	13.0	5.99	12.34	2.50	0.36
	2,514	2,416	736.4	49.7	2.42	15.7	12.9	4.81	11.02	2.49	0.33
	2,506	2,424	738.8	46.8	2.30	14.9	13.8	5.51	13.16	2.44	0.37
	2,484	2,446	745.5	48.2	2.11	15.3	13.5	4.94	12.68	2.37	0.38
	2,462	2,468	752.2	48.2	2.41	15.3	13.4	5.51	11.69	2.43	0.33
	2,448	2,482	756.5	47.5	1.94	15.1	12.8	9.68	9.93	2.08	0.39
	2,418	2,512	765.7	48.0	1.98	15.1	11.8	9.68	10.22	2.11	0.40
	2,348	2,582	787.0	49.9	2.44	14.6	13.1	4.70	10.67	2.89	1.08
	2,321	2,609	795.2	50.0	2.23	14.5	13.5	5.63	9.05	3.08	1.40

* Total iron reported as FeO.

Source: 1996-97 data, ISU Geochemistry Lab.

Table 4-7. Major element geochemical data for Well WO-2.

Well	Elev. (ft)	Depth (ft)	Depth (m)	SiO2	TiO2	Al2O3	FeO*	MgO	CaO	Na2O	K2O
WO-2											
	4,910	20	6.1	48.3	2.82	15.4	13.1	6.46	9.34	2.92	0.94
	4,853	77	23.5	48.2	2.25	16.7	13.2	5.53	9.40	3.00	0.71
	4,840	90	27.4	47.6	2.70	14.5	13.5	8.19	9.84	2.53	0.63
	4,742	188	57.3	46.8	2.63	14.8	13.3	7.98	10.08	2.69	0.83
	4,581	349	106.4	47.8	1.87	15.7	11.7	8.39	11.11	2.47	0.43
	4,499	431	131.4	47.5	1.15	16.6	10.1	10.55	11.49	2.20	0.19
	4,304	626	190.8	47.3	2.20	14.9	12.9	9.06	10.32	2.39	0.45
	4,275	655	199.6	47.4	2.21	15.2	12.6	8.78	10.58	2.40	0.45
	4,225	705	214.9	48.0	2.10	15.2	12.2	8.82	10.14	2.36	0.66
	4,144	786	239.6	47.1	2.38	15.4	13.1	8.28	10.01	2.55	0.66
	4,070	860	262.1	48.3	2.40	15.5	12.7	7.43	9.56	2.77	0.86
	4,003	927	282.5	46.5	2.44	15.3	13.0	8.78	10.06	2.56	0.63
	3,986	944	287.7	47.7	3.24	14.5	14.4	6.52	9.59	2.56	0.67
	3,932	998	304.2	47.3	2.37	15.0	12.8	8.89	10.18	2.42	0.55
	3,920	1,010	307.8	48.0	2.64	14.6	13.6	7.73	9.44	2.58	0.79
	3,876	1,054	321.3	47.9	2.82	15.2	13.5	7.33	9.48	2.20	0.81
	3,856	1,074	327.4	48.0	2.93	14.5	13.6	7.24	9.67	2.57	0.79
	3,808	1,122	342.0	49.5	2.26	15.8	11.7	6.75	9.23	2.95	1.03
	3,794	1,136	346.3	48.9	2.09	18.0	11.8	5.44	9.59	2.96	0.91
	3,766	1,164	354.8	48.1	2.83	14.5	13.7	7.09	9.61	2.65	0.85
	3,709	1,221	372.2	47.5	2.82	15.0	13.8	7.13	10.08	2.44	0.65
	3,691	1,239	377.6	47.1	2.95	14.4	14.3	7.42	9.69	2.58	0.75
	3,667	1,263	385.0	48.0	1.96	16.2	11.8	8.30	9.86	2.67	0.66
	3,644	1,286	392.0	47.4	2.30	14.7	12.9	9.04	10.02	2.40	0.64
	3,640	1,290	393.2	47.4	2.35	14.8	13.2	8.48	10.18	2.44	0.56
	3,626	1,304	397.5	48.1	2.45	15.0	12.8	7.89	10.14	2.46	0.64
	3,614	1,316	401.1	47.9	1.98	15.2	12.5	9.07	10.19	2.33	0.53
	3,552	1,378	420.0	47.0	2.27	14.5	13.4	9.49	9.86	2.35	0.57
	3,450	1,480	451.1	47.0	2.42	16.3	14.5	6.23	9.40	2.81	0.47
	3,389	1,541	469.7	48.0	2.04	14.8	12.2	9.35	10.57	2.28	0.39
	3,365	1,565	477.0	48.4	2.95	15.9	11.7	6.45	9.77	3.08	0.89
	3,331	1,599	487.4	48.1	1.74	15.4	11.4	8.69	11.18	2.40	0.60
	3,298	1,632	497.4	48.4	1.95	15.2	12.0	9.01	9.84	2.53	0.63
	3,199	1,731	527.6	45.9	3.45	14.2	15.4	7.33	10.11	2.53	0.35
	3,125	1,805	550.2	47.8	3.01	14.2	14.4	7.52	9.65	2.32	0.54
	3,067	1,863	567.8	47.2	2.45	14.9	13.0	8.23	10.53	2.43	0.52
	3,027	1,903	580.0	46.9	2.81	14.6	14.2	8.04	10.00	2.37	0.46
	2,880	2,050	624.8	47.0	2.89	14.3	14.1	7.34	10.95	2.32	0.41
	2,839	2,091	637.3	46.7	3.03	15.1	14.1	7.03	10.52	2.46	0.43

Table 4-7. (continued).

Well	Elev. (ft)	Depth (ft)	Depth (m)	SiO2	TiO2	Al2O3	FeO*	MgO	CaO	Na2O	K2O
WO-2											
	2,740	2,190	667.5	46.9	2.75	15.6	15.2	6.00	10.01	2.44	0.39
	2,732	2,198	670.0	48.2	3.18	16.1	13.4	5.92	10.64	1.48	0.65
	2,605	2,325	708.7	47.2	3.03	15.1	13.8	7.51	10.04	2.28	0.41
	2,472	2,458	749.2	47.2	2.09	15.3	12.6	8.72	10.90	2.39	0.30
	2,431	2,499	761.7	47.0	3.02	14.6	14.5	7.74	10.13	2.17	0.16
	2,355	2,575	784.9	50.4	3.43	12.3	14.8	8.60	5.78	1.46	2.65
	2,319	2,611	795.8	46.7	2.90	14.5	15.3	7.42	9.74	2.32	0.28
	2,223	2,707	825.1	52.8	2.22	14.0	11.7	6.14	8.42	2.57	1.59
	2,148	2,782	848.0	47.4	3.26	13.8	14.9	6.52	10.54	2.49	0.42
	2,052	2,878	877.2	48.4	2.93	14.3	15.0	5.67	9.24	2.60	0.57
	1,930	3,000	914.4	47.4	2.73	13.7	15.0	7.20	10.66	2.38	0.29
	1,851	3,079	938.5	46.5	3.35	14.4	15.4	7.09	10.17	2.38	0.23
	1,737	3,193	973.2	48.3	2.01	15.2	12.0	8.99	9.87	2.46	0.62
	1,688	3,242	988.2	46.9	3.39	14.2	14.7	7.17	9.90	2.18	0.68
	1,589	3,341	1,018.3	47.3	1.43	17.9	12.2	7.93	9.76	2.88	0.36
	1,521	3,409	1,039.1	48.7	1.64	16.2	12.2	7.67	10.27	2.75	0.35
	1,324	3,606	1,099.1	50.8	1.17	15.1	10.2	8.83	10.64	2.48	0.57
	1,285	3,645	1,111.0	51.1	1.95	14.8	12.6	4.97	9.82	3.20	1.20
	1,190	3,740	1,140.0	48.3	2.00	15.2	12.1	8.71	10.30	2.45	0.58

* Total iron reported as FeO.
Original Source: John Shervais and Scott Vetter, University of South Carolina.
NOTE: *Data was obtained from the ISU ESRP geochemistry database.*

Table 4-8. Major element geochemical data for Well C1A.

Well	Elev. (ft)	Depth (ft)	Depth (m)	SiO2	TiO2	Al2O3	FeO*	MgO	CaO	Na2O	K2O
C1A											
	4,724	301	91.7	48.1	1.52	15.9	10.1	9.83	11.30	2.32	0.49
	4,697	328	100.0	48.2	1.22	16.1	10.6	9.36	11.89	2.15	0.13
	4,690	335	102.1	48.8	1.37	16.3	8.3	11.32	11.21	1.87	0.43
	4,684	341	103.9	48.3	1.20	16.0	10.1	10.00	11.62	2.24	0.18
	4,674	351	107.0	47.9	1.19	16.3	10.5	9.90	11.57	2.21	0.16
	4,637	388	118.3	47.2	1.19	16.2	10.5	10.47	11.70	2.16	0.20
	4,624	401	122.2	46.9	3.44	13.8	15.1	6.22	9.90	2.45	0.86
	4,611	414	126.2	46.9	3.12	14.5	14.5	6.72	9.80	2.47	0.83
	4,574	451	137.5	47.3	2.90	14.7	14.0	7.24	9.67	2.46	0.83
	4,562	463	141.1	47.3	2.88	14.6	13.7	7.42	9.65	2.55	0.99
	4,540	485	147.8	47.8	2.97	14.4	13.8	7.14	9.61	2.63	0.84
	4,529	496	151.2	47.5	2.79	14.7	13.8	7.30	9.69	2.52	0.78
	4,518	507	154.5	47.7	2.79	14.7	13.7	7.31	9.68	2.60	0.72
	4,503	522	159.1	47.6	2.78	14.7	13.7	7.53	9.73	2.57	0.69

Table 4-8. (continued).

Well	Elev. (ft)	Depth (ft)	Depth (m)	SiO2	TiO2	Al2O3	FeO*	MgO	CaO	Na2O	K2O
C1A											
	4,479	546	166.4	47.5	2.67	15.0	13.6	7.47	9.80	2.54	0.70
	4,444	581	177.1	48.9	1.53	16.4	10.2	9.12	10.71	2.38	0.38
	3,835	1,190	362.7				13.2			2.46	
	3,981	1,044	318.2				12.2			2.34	
	3,711	1,314	400.5				12.9			2.77	
	3,406	1,619	493.5				13.5			1.75	
	3,248	1,777	541.6				15.8			2.27	

* Total iron reported as FeO.
Source: 1997 data, Paul Wetmore, ISU thesis, ISU Geochemistry Lab (Wetmore 1998).

Table 4-9. Minor element geochemical data for Well 2-2A.

Well	Elevation (ft) MSL	Depth (ft)	Depth (m)	Ni (ppm)	Zn (ppm)	Sr (ppm)	Elevation (ft) MSL	Depth (ft)	Depth (m)	Ni (ppm)	Zn (ppm)	Sr (ppm)
2-2A												
	4,885	45	13.7	65	136	300	3,646	1,284	391.4	100	—	354
	4,876	54	16.5	56	140	305	3,628	1,302	396.8	—	—	357
	4,664	266	81.1	105	146	268	3,606	1,324	403.6	85	—	331
	4,632	298	90.8	61	154	278	3,595	1,335	406.9	100	—	354
	4,597	333	101.5	76	124	282	3,355	1,575	480.1	75	—	264
	4,578	352	107.3	53	162	289	3,317	1,613	491.6	100	—	242
	4,537	393	119.8	100		266	3,153	1,777	541.6	—	—	275
	4,508	422	128.6	85		319	3,019	1,911	582.5	—	—	344
	4,487	443	135.0	105	179	324	3,003	1,927	587.3	125	160	316
	4,468	462	140.8	83	169	323	2,984	1,946	593.1	—	142	346
	4,448	482	146.9	58	132	328	2,946	1,984	604.7	75	113	236
	4,435	495	150.9	65	138	326	2,927	2,003	610.5	50	137	299
	4,417	513	156.4	90	150	327	2,907	2,023	616.6	60	152	271
	4,387	543	165.5	64	138	337	2,891	2,039	621.5	90	156	274
	4,344	586	178.6	89	136	345	2,854	2,076	632.8	85	146	250
	4,322	608	185.3	78	160	325	2,834	2,096	638.9	95	129	254
	4,312	618	188.4	86	150	336	2,790	2,140	652.3	100	145	243
	4,275	655	199.6	155	113	220	2,774	2,156	657.1	95	123	254
	4,264	666	203.0	150	117	221	2,729	2,201	670.9	115	103	246
	4,252	678	206.7	155	91	223	2,706	2,224	677.9	90	118	285
	4,213	717	218.5	150	88	223	2,661	2,269	691.6	85	86	227
	4,174	756	230.4	76	127	276	2,625	2,305	702.6	100	—	245
	4,160	770	234.7	100	136	277	2,603	2,327	709.3	105	99	274
	4,151	779	237.4	115	119	240	2,581	2,349	716.0	190	59	199
	4,122	808	246.3	100	118	238	2,576	2,354	717.5	170	—	228

Table 4-9. (continued).

Well	Elevation (ft) MSL	Depth (ft)	Depth (m)	Ni (ppm)	Zn (ppm)	Sr (ppm)	Elevation (ft) MSL	Depth (ft)	Depth (m)	Ni (ppm)	Zn (ppm)	Sr (ppm)
	4,109	821	250.2	95	131	247	2,553	2,377	724.5	100	—	283
	4,087	843	256.9	85	118	223	2,538	2,392	729.1		165	333
	4,021	909	277.1	110	111	328	2,527	2,403	732.4		160	365
	4,000	930	283.5	110	129	324	2,514	2,416	736.4		139	342
	3,975	955	291.1	90		266	2,506	2,424	738.8		160	345
	3,760	1,170	356.6			326	2,484	2,446	745.5		152	368
	3,740	1,190	362.7	90	161	324	2,462	2,468	752.2		170	343
	3,718	1,212	369.4	73	131	314	2,448	2,482	756.5		82	222
	3,696	1,234	376.1	95	163	352	2,418	2,512	765.7		60	221
	3,688	1,242	378.6	90		348	2,348	2,582	787.0		225	318
	3,661	1,269	386.8	66		346	2,321	2,609	795.2		159	284

Source: 1996-97 data, ISU Geochemistry Lab.

Table 4-10. Minor element geochemical data for Well WO-2.

Well	Elevation (ft) MSL	Depth (ft)	Depth (m)	Ni (ppm)	Zn (ppm)	Sr (ppm)	Elevation (ft) MSL	Depth (ft)	Depth (m)	Ni (ppm)	Zn (ppm)	Sr (ppm)
WO-2												
	4,910	20	6.1	53	122	318	3,389	1,541	469.7	130	96	222
	4,853	77	23.5	84	115	305	3,365	1,565	477.0	97	113	287
	4,840	90	27.4	105	114	294	3,331	1,599	487.4	101	96	235
	4,742	188	57.3	58	120	291	3,298	1,632	497.4	133	104	239
	4,581	349	106.4	118	95	217	3,199	1,731	527.6	83	135	288
	4,499	431	131.4	157	71	194	3,125	1,805	550.2	114	131	315
	4,304	626	190.8	86	104	266	3,067	1,863	567.8	97	115	266
	4,275	655	199.6	80	101	264	3,027	1,903	580.0	107	118	275
	4,225	705	214.9	135	100	272	2,880	2,050	624.8	49	129	280
	4,144	786	239.6	132	106	285	2,839	2,091	637.3	70	121	332
	4,070	860	262.1	219	112	264	2,740	2,190	667.5	66	131	318
	4,003	927	282.5	145	110	274	2,732	2,198	670.0	63	134	241
	3,986	944	287.7	78	137	311	2,605	2,325	708.7	128	120	334
	3,932	998	304.2	124	99	254	2,472	2,458	749.2	83	92	264
	3,920	1,010	307.8	93	126	301	2,431	2,499	761.7	113	129	279
	3,876	1,054	321.3	112	114	297	2,355	2,575	784.9	105	144	266
	3,856	1,074	327.4	116	121	282	2,319	2,611	795.8	107	130	290
	3,808	1,122	342.0	119	111	288	2,223	2,707	825.1	49	102	225
	3,794	1,136	346.3	51	118	301	2,148	2,782	848.0	76	134	306
	3,766	1,164	354.8	57	120	299	2,052	2,878	877.2	75	131	321
	3,709	1,221	372.2	69	122	313	1,930	3,000	914.4	93	128	320

Table 4-10. (continued).

Well	Elevation (ft) MSL	Depth (ft)	Depth (m)	Ni (ppm)	Zn (ppm)	Sr (ppm)	Elevation (ft) MSL	Depth (ft)	Depth (m)	Ni (ppm)	Zn (ppm)	Sr (ppm)
	3,691	1,239	377.6	71	117	306	1,851	3,079	938.5	96	131	334
	3,667	1,263	385.0	139	100	259	1,737	3,193	973.2	93	128	314
	3,644	1,286	392.0	134	115	253	1,688	3,242	988.2	86	143	283
	3,640	1,290	393.2	129	116	256	1,589	3,341	1,018.3	74	82	316
	3,626	1,304	397.5	75	109	310	1,521	3,409	1,039.1	110	97	256
	3,614	1,316	401.1	117	98	251	1,324	3,606	1,099.1	181	86	230
	3,552	1,378	420.0	82	107	263	1,285	3,645	1,111.0	61	118	273
	3,450	1,480	451.1	104	122	272	1,190	3,740	1,140.0	89	105	246

Original Source: John Shervais and Scott Vetter, University of South Carolina.
NOTE: *Data was obtained from the ISU ESRP geochemistry database.*

Table 4-11. Minor element geochemical data for Well C1A.

Well	Elevation (ft) MSL	Depth (ft)	Depth (m)	Ni (ppm)	Zn (ppm)	Sr (ppm)	Elevation (ft) MSL	Depth (ft)	Depth (m)	Ni (ppm)	Zn (ppm)	Sr (ppm)
C1A												
	4,724	301	91.7	175	61	209	4,529	496	151.2	102	151	357
	4,697	328	100.0	180	68	176	4,518	507	154.5	46	129	355
	4,690	335	102.1	64	38	212	4,503	522	159.1	89	138	351
	4,684	341	103.9	104	55	173	4,479	546	166.4	99	152	361
	4,674	351	107.0	118	65	174	4,444	581	177.1	165	53	245
	4,637	388	118.3	120	54	177	3,981	1,044	318.2		112	255
	4,624	401	122.2	90	195	344	3,835	1,190	362.7	88	178	260
	4,611	414	126.2	105	149	355	3,711	1,314	400.5		150	200
	4,574	451	137.5	80	164	354	3,406	1,619	493.5		135	320
	4,562	463	141.1	91	163	350	3,248	1,777	541.6		500	240
	4,540	485	147.8	86	162	345						

Source: 1997 data, Paul Wetmore, ISU thesis, ISU Geochemistry Lab (Wetmore 1998).

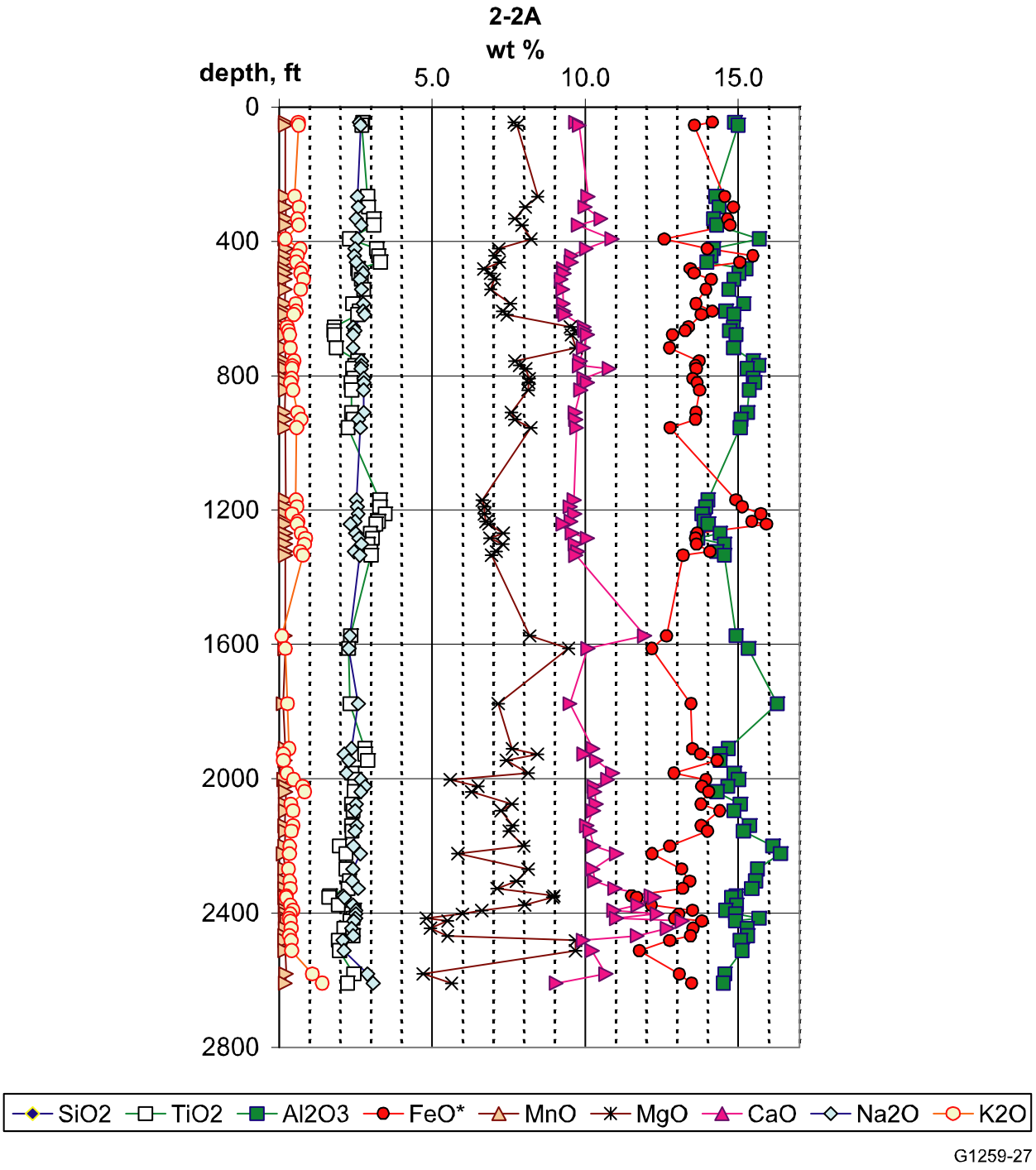

a. Major element oxides for Well 2-2A.

NOTE: *The basalts immediately below the Olduvai Lake Beds start just above 1,200 ft bls. In the pre-Olduvai basalts, values for iron as FeO start at approximately 15%, rise to 15.9%, and then drop to >14% in the 200-ft interval immediately below the Olduvai Subchron sediments. (* = Total iron is reported as FeO.)*

Figure 4-7. Major element concentrations as oxides of pre-Olduvai basalts.

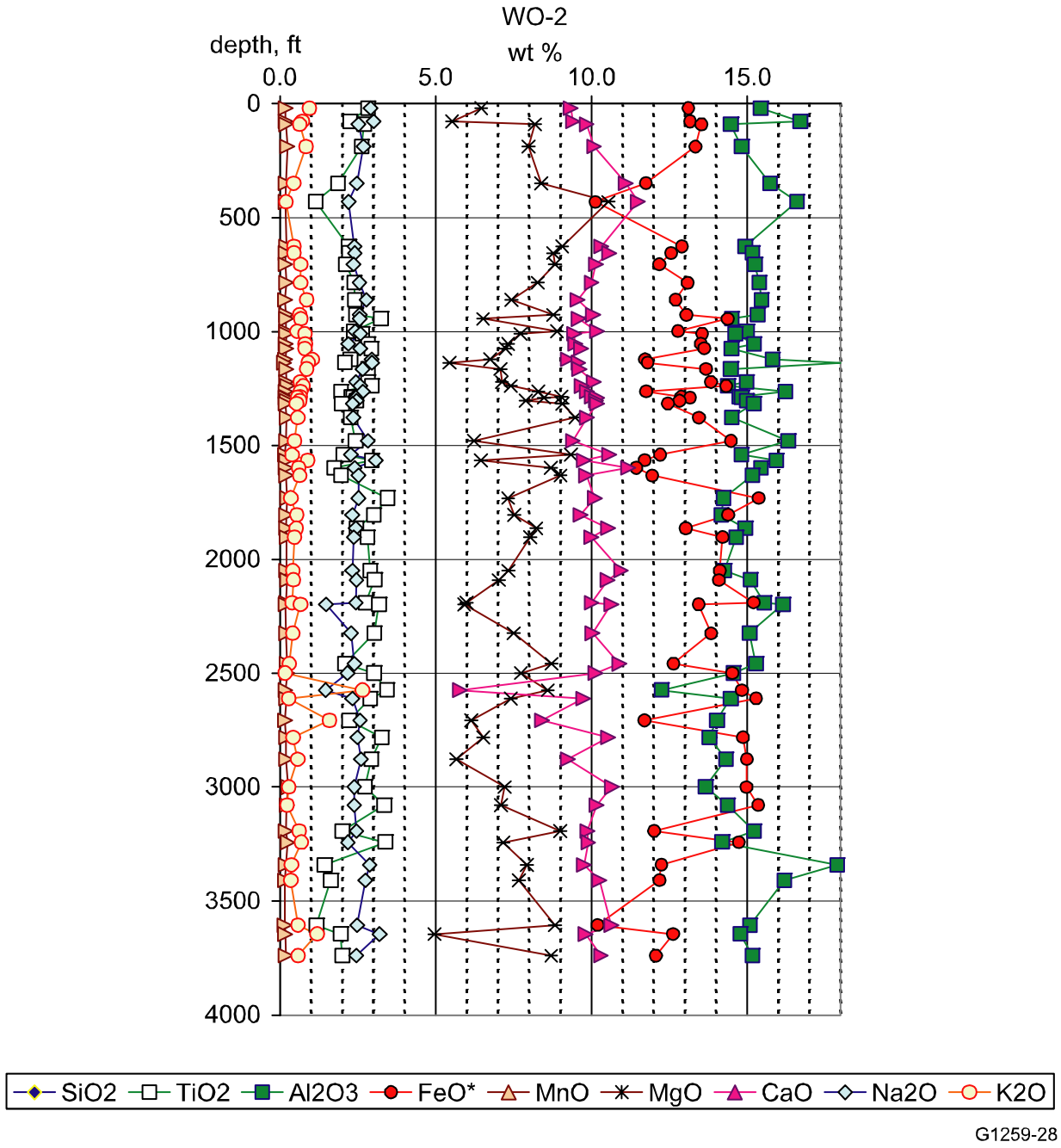

b. Major element oxides for Well WO-2.

NOTE: *The basalts immediately below the Olduvai Lake Beds start at ~1,800 ft bls. The basalt at 1,730 ft bls, dated at 1.856 Ma (Anderson and Liszewski 1997), is at the local maximum for iron as an oxide. This basalt is sandwiched between Olduvai Lake sediments above and below. (* = Total iron is reported as FeO.)*

Figure 4-7. (continued).

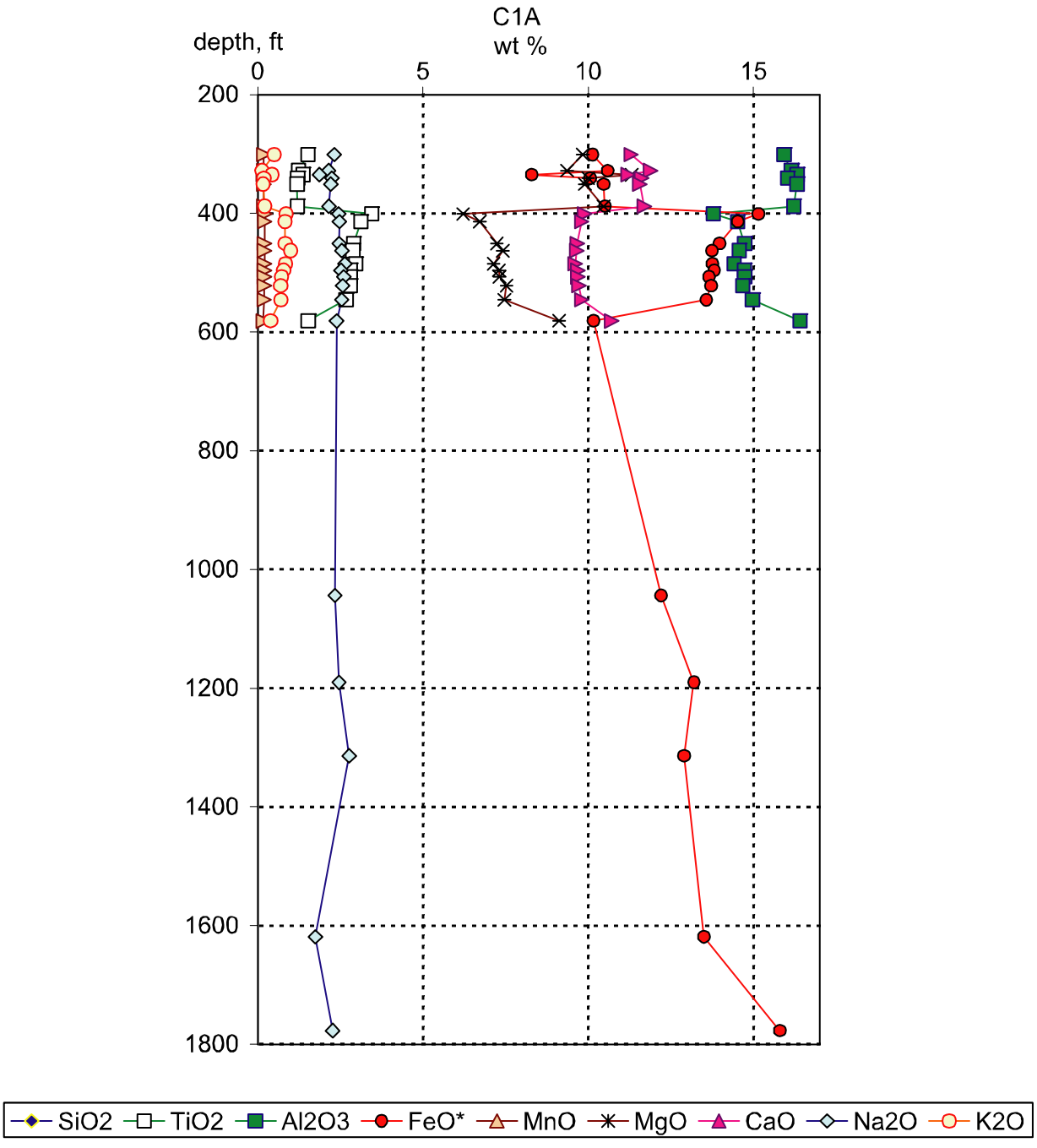

c. Major element oxides for Well C1A.

NOTE: *The iron and sodium concentrations of the basalt at 1,777 ft bls match those of the pre-Olduvai basalts immediately below the Olduvai Lake sediments in Wells 2-2A and WO-2. (* = Total iron is reported as FeO.)*

Figure 4-7. (continued).

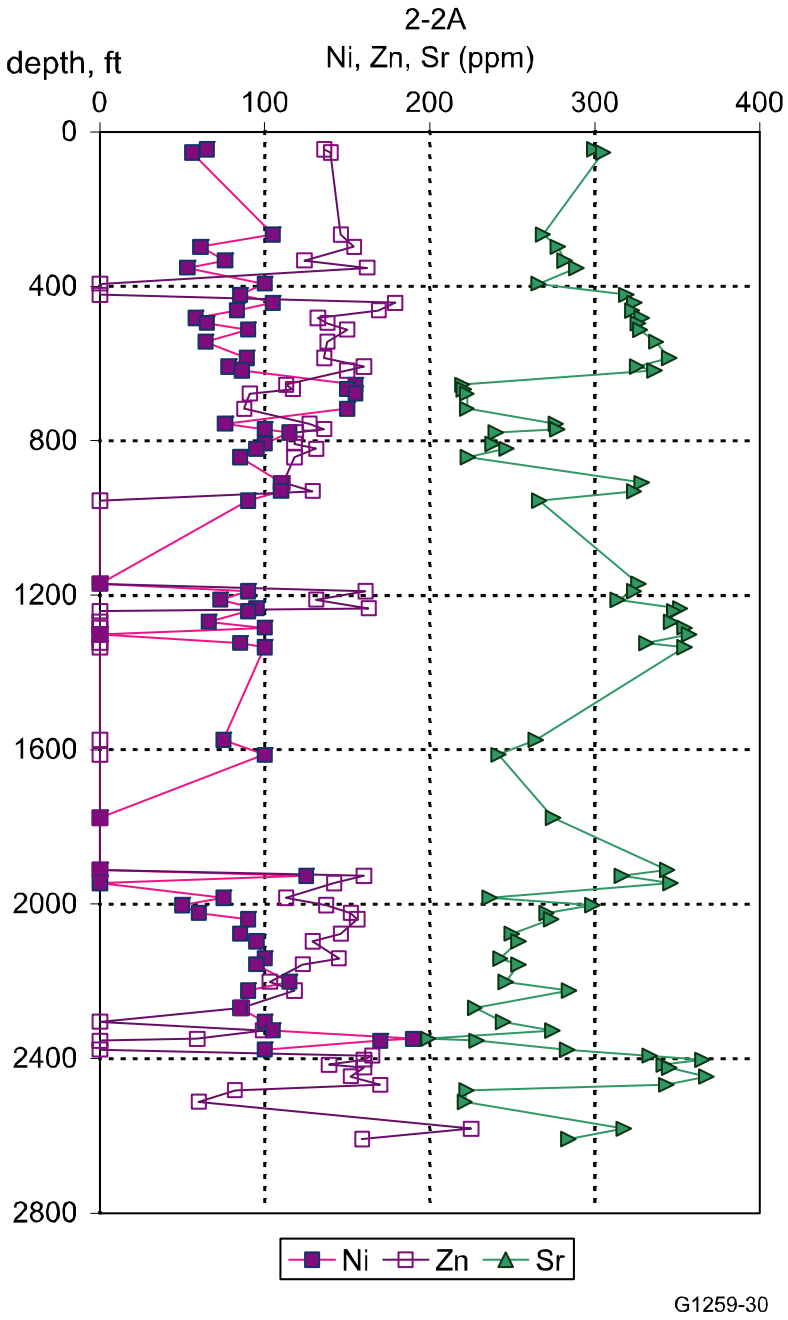

a. Minor element concentrations for Well 2-2A.

NOTE: *The basalts immediately below the Olduvai Lake Beds first occur just above 1,200 ft bls.*

Figure 4-8. Minor element concentrations of Ni, Zn, and Sr of pre-Olduvai basalts.

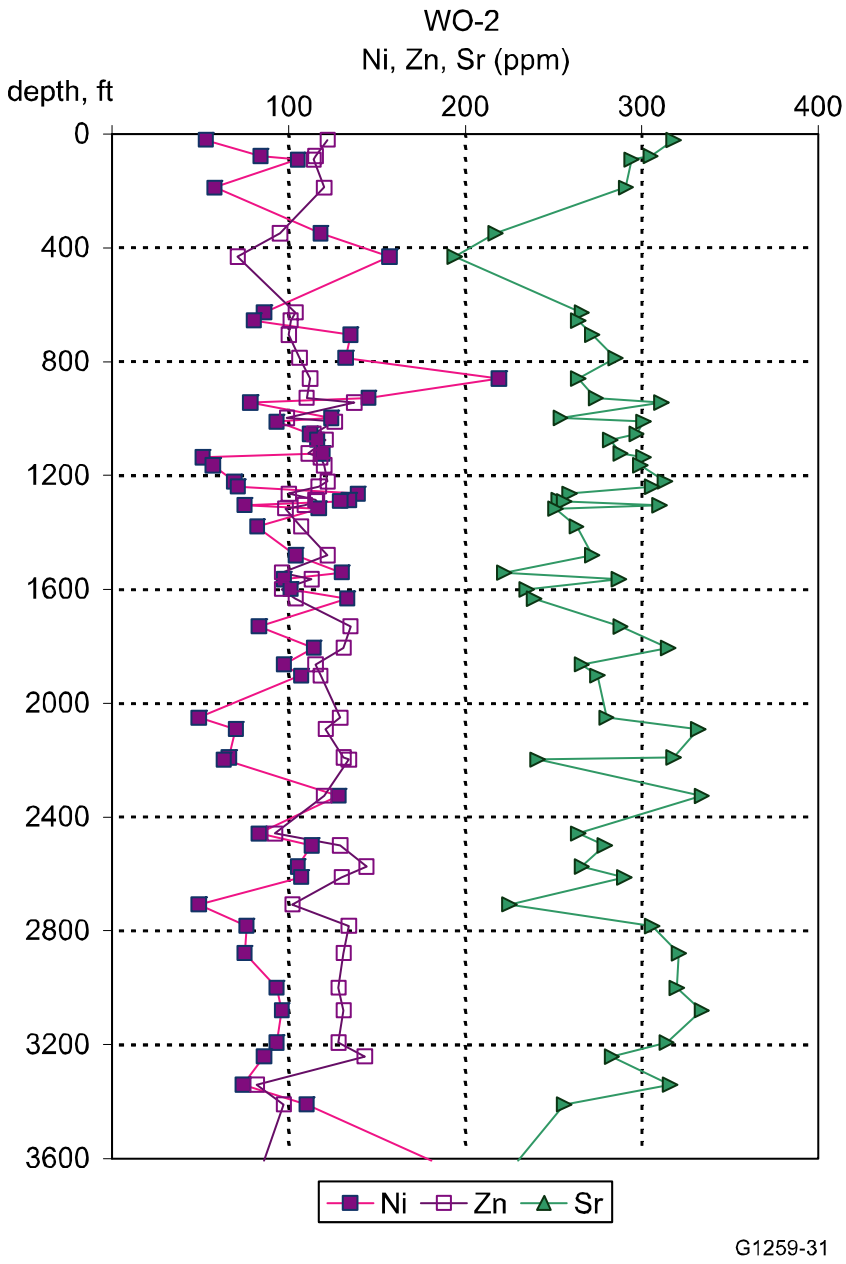

b. Minor element concentrations for Well WO-2.

NOTE: *The basalts immediately below the Olduvai Lake Beds first occur at ~1,800 ft bls.*

Figure 4-8. (continued).

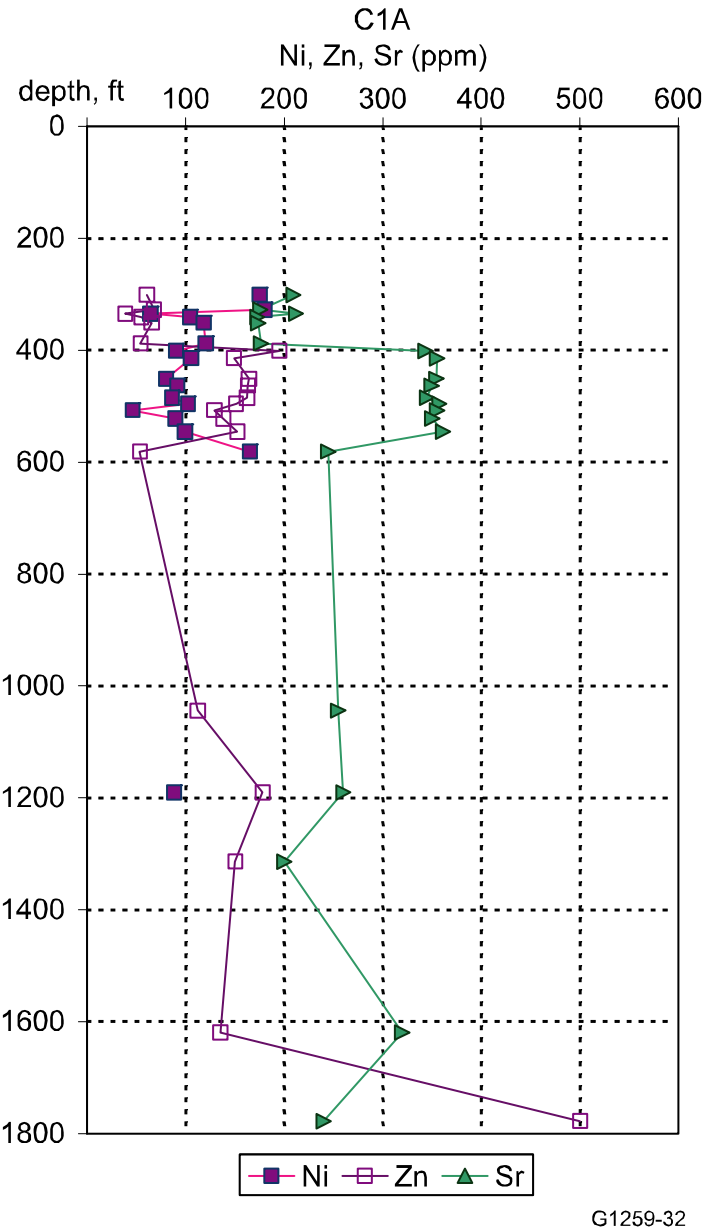

c. Minor element concentrations for Well C1A.

NOTE: *The concentrations of the basalt at 1,777 ft bls do not match those of the pre-Olduvai basalts immediately below the Olduvai Lake sediments in Wells 2-2A and WO-2, although the alteration state of this deep basalt in Well C1A is unknown.*

Figure 4-8. (continued).

Geochemical profiling might help determine the geochronology of the deep strata cored at the Site. Similarities or the lack thereof in geochemical trends for C1A, WO-2, and 2-2A could help to identify the location of Jaramillo vs. Olduvai or pre-Olduvai basalts. The similarities in geochemical profiles of the pre-Olduvai basalts from 2-2A and WO-2 demonstrate that this sort of analysis could be fruitful.

The datasets available for the deeper portions of C1A are geophysical logs and a handful of geochemical analyses from the ISU database. The deepest geochemical data in C1A, at 1,777 ft bls, resembles the geochemistry of the pre-Olduvai basalts in 2-2A and WO-2 (see Figures 4-7 and 4-8). Iron as an oxide is 15.8% and sodium is 2.3%. There are no other major element analyses available, however. The trace element values for Zn are 500 ppm and for Sr are 240 ppm—not values that match the pre-Olduvai basalts in 2-2A and WO-2. Unfortunately, deep in C1A, the sample density is so low that we cannot look at trends in concentrations here as we can in the other two wells. So, while the sparse major element chemistry suggests that the basalt at 1,777 ft bls in C1A might be near and below the stratigraphic position of the Olduvai Beds, the trace element chemistry argues otherwise.

We could possibly explain the trace element data by pointing out that trace element concentrations are susceptible to low-grade alteration, especially as depth increases toward the base of the aquifer. This is difficult to support, however, because extrapolating from such sparse data is not really defensible. An additional difficulty is presented by the mobility of elements during alteration, since alteration that mobilizes trace elements like Sr and Zn also usually has mobilized the major elements (Rollinson 1993). Although the unpublished age date for the third normal polarity interval in C1A argues for a much deeper location for the Olduvai Lake, the correlation of the 1,777-ft basalt in C1A with the high-iron, pre-Olduvai basalts in 2-2A and WO-2 argues that more data is required to resolve the questions posed by correlating the deepest strata penetrated at INL.

5. DISCUSSION AND CONCLUSION

5.1 The Relationship of Middle-1823 to Local Stratigraphy

Like many other boreholes near TRA and INTEC, Middle-1823 strata above ~500 ft bls cannot only be correlated to interbeds and basalts locally, but can be correlated at depth to units between 500 and 1,500 ft bls north as far as Well TRA-5 and possibly south to Well C1A. Shallow correlations with sediments and one basalt flow group with an age between 414 and 643 ka can be made from Middle-1823 north to Site-19, south to ICPP-SCI-V-214, and east to USGS-84. East-west correlations are difficult in this area, due to the interfingering of units under the Big Lost flood plain and the data gap between TRA and INTEC. At depth, the sequence of thick interbeds in the subaquifer zone of Middle-1823 can be correlated to the thick sequence of deep interbeds in the bottom of TRA-5 and potentially to the deep interbeds in INEL-1, WO-2, and 2-2A, if found to belong to the Olduvai Subchronozone, or it can be correlated to the deep interbeds in C1A if found to belong to the Jaramillo Subchronozone. No correlations above the deep interbeds are possible on the west side of the flood plain north of Site-19 and MTR-Test at TRA, and on the east side of the flood plain north of USGS-121 at INTEC. The inability to correlate is due to (a) extensive interfingering in the subsurface under the flood plain, (b) disruption of the local stratigraphy by the northwest-trending AEC Butte volcanic rift zone, and (c) the lack of data for wells between AEC Butte and the NRF area.

5.1.1 The I-Flow

The published intervals for the USGS I-Flow (Anderson et al. 1996) are not correct outside of the INTEC area. The I-Flow depths for most of the INTEC wells consistently pick a two-part flow group with an age of 641 ka and a slightly elevated NGR response in comparison to flows above and below. The I-Flow picks at TRA, however, vary from the TRA-B6 basalt in USGS-80 to a flow 150 ft deeper than TRA-B6 in USGS-58, and to flows that are 200 ft deeper than TRA-B6 in TRA-5 and TRA-6A. The I-Flow pick for USGS-76 is 250 ft deeper than the base of the basalt in the equivalent position at TRA-B6. In USGS-76, the I-Flow pick is capped by and includes an interbed with sand and clay. The top of the I-Flow picks in USGS-58, TRA-5, and TRA-6A are all capped with an intertrappean layer containing “cinders.” All of these capping layers have either cinders or clay in them, both of which typically cause a local maximum in NGR counts. It is likely, therefore, that the TRA I-Flow picks were chosen on the basis of NGR shape matching and were possibly biased by anticipating where the top of the I-Flow would be if the I-Flow was really the same unit at both INTEC and TRA. The USGS I-Flow picks at TRA and points south were not an unreasonable interpretation at the time they were made. The geochemical data suggesting that the 643 and 641 ka basalts at TRA and INTEC, respectively, are from different sources were not available when the original analysis of the I-Flow was formulated. Many of the age dates available for INTEC and TRA basalts today also were not available at that time. Clearly, this situation underscores the need to update the Site stratigraphy models continuously and rigorously, as new datasets for INL basalts become available.

We believe that newly available datasets for the TRA and INTEC areas support a scenario where the INTEC I-Flow and the Basalt of AEC belong to different flow groups with distinctly different magmatic sources. This has consequences for Site stratigraphy as presented in recent USGS publication such as Anderson and Liszewski (1997), since the coherence of the composite stratigraphic packages like Unit 7 (which includes the USGS I-Flow) cannot be maintained in northwest to southeast transects across the flood plain. The current “state of the data” supports discontinuity of units across the flood plain, not coherence.

5.1.2 The Big Lost Trough versus the Big Lost Syncline

The analyses of Blair (2002), Blair and Link (2000), Anderson and Liszewski (1997), Champion et al. (2002) and others have made a case for the existence of a subsurface depression under and slightly to the east of the Big Lost flood plain. This trough model depends in part on the character of composite stratigraphic packages whose strata share certain hydrological characteristics, like omnibus Unit 7 dominated by a massive low-to-moderate permeability I-Flow, based on properties inferred for the 641 ka flow at INTEC and NPR. The geometry of the trough model also depends on the inferred position of the Olduvai Lake Beds in C1A compared to their position in wells such as WO-2. Placing the Olduvai beds at 3,640 ft MSL in C1A was based on the assumption that the normal polarity interval from ~1,100 to ~1,450 ft bls in C1A was the Olduvai Subchron. We now know that these assumptions about the I-Flow and the placement of the Olduvai Beds in C1A might be incorrect based on new data that has become available since the I-Flow and Big Lost Trough models were conceived. Based on age dates, paleomagnetic inclinations, and geochemical profiling, a good case can be made that the 641 ka basalt at INTEC does not correlate with Anderson et al.'s (1996) I-Flow picks in the TRA well field or with the position of the Basalt of AEC Butte. The new C1A age date of 820 ka ± 160 ka at 1,195 ft bls (Helm-Clark and Rodgers 2004) suggests that the normal polarity basalts from ~1,100 to ~1,450 ft bls belong to the Jaramillo Subchronozone, an inference that is potentially supported by preliminary paleomagnetic data locating the Jaramillo interval in Middle-1823. The results of these new data support an interpretation that pushes the position of the Olduvai Subchronozone to below ~1,800 ft bls in C1A and modifies the 2-2A/WO-2/C1A stratigraphic profile from a trough to a southward-dipping syncline.

5.1.3 Critical Data Needs and Recommendations

Geophysical logs for NGR, N, and temperature should be collected for the Fire Station Well (FSW) (Figure 4-4). The same set of logs should be collected for TRA-2 (Figure 4-1).

Future coring and logging efforts should attempt to emulate the logging and coring program followed by the borehole geophysics group from USGS Denver for Well ANL-OBS-A-001 (Paillet and Boyce 1996) at the Argonne National Laboratory-West facility (Figure 1-1). The Paillet and Boyce (1996) drilling strategy involves the cessation of drilling when collapsing formations are encountered in order to collect a caliper log in the open hole. Then, the collapsed interval is either grouted or cased to keep the borehole open through the collapsing interval. Drilling resumes following grouting or casing. This strategy would enable the collection and proper interpretation of a density log, which is not possible without a caliper log.

Paleomagnetic inclination data are actually one of the most powerful tools available for establishing correlations. In places like TRA, where we know the shallow basalts are already as old as >400 ka, paleomagnetic data is crucial for locating the Big Lost paleomagnetic excursion, the Jaramillo and Olduvai Subchrons, and the Bruhnes-Matayuma transition. Because of the value and utility of these data, coring from the surface is highly recommended for all research boreholes. Collecting a good set of cores also makes it possible to sample for geochemical profiling, which is perhaps the best new tool we have to establish and clarify correlations. The disadvantage, however, is that coring and geochemistry analyses are expensive.

The largest data need is for subsurface information in the TRA-INTEC data gap. This gap exists between USGS-80 and USGS-121 to the north, USGS-84 and USGS-39 to the south, and USGS-66 and USGS-43 in between (Figure 4-1). While extra boreholes north of the AEC Butte rift zone would be extremely useful, logging the Fire Station Well (Figure 4-4) should be completed first so an informed decision about drilling in that area can be made. The best place for a new research borehole would be either between USGS-80 and USGS-121 or in the center of the polygon bounded by Wells USGS-66,

USGS-43, USGS-39, and USGS-84. Since a well located in the center of this polygon would close the larger of these two data gaps, this location probably should take precedence over the more northern one. Any future borehole drilled for research purposes should be cored from the surface, and the cores should be analyzed for paleomagnetic, geochemical, and radiometric age data. Within the realm of practicality, a complete set of geophysical logs should be collected, including caliper and temperature data, even if this involves drilling and casing the hole in stages in the manner of Paillet and Boyce (1996).

6. REFERENCES

Anderson, S. R., and R. C. Bartholomay, 1995, "Use of natural-gamma logs and cores for determining stratigraphic relations of basalt and sediment at the Radioactive Waste Management Complex, Idaho National Engineering Laboratory, Idaho," *Journal of the Idaho Academy of Science,* Vol. 31 (1), pp. 1–10.

Anderson, S. R., and M. J. Liszewski, 1997, *Stratigraphy of the Unsaturated Zone and Snake River Plain Aquifer at and near the Idaho National Engineering Laboratory*, *Idaho,* U.S. Geological Survey Water Resources Investigation Report 97-4183.

Anderson, S. R., D. J. Ackerman, M. J. Liszewski, and R. M. Freiburger, 1996, *Stratigraphic Data for Wells at and near the Idaho National Engineering Laboratory*, *Idaho*, DOE/ID-22127, U.S. Geological Survey Open-File Report 96-248.

Anderson, S. R., M. A. Kuntz, and L. C. Davis, 1999, *Geologic Controls of Hydraulic Conductivity in the Snake River Plain Aquifer at and near the Idaho National Engineering and Environmental Laboratory, Idaho*, U.S. Geological Survey Water Resources Investigation Report 99-4033.

Anderson, S. R., M. J. Liszewski, and L. D. Cecil, 1997, *Geologic Ages and Accumulation Rates of Basalt Flow Groups and Sedimentary Interbeds in Selected Wells at the Idaho National Engineering Laboratory, Idaho*, U.S. Geological Survey Water Resources Investigation Report 97-4010.

Bestland, E. A., P. K. Link, D. Champion, and M. Lanphere, 2002, "Paleoenvironments of sedimentary interbeds in the Pliocene-Pleistocene Big Lost Trough (Eastern Snake River Plain, Idaho)," Link, P. K., and L. L. Mink, eds., *Geology, Hydrogeology, and Environmental Remediation, Idaho National Engineering and Environmental Laboratory, Eastern Snake River Plain*, Geological Society of America Special Paper 353.

Blair, J. J., 2002, *Sedimentology and Stratigraphy of Sediments of the Big Lost Trough Subsurface from Selected Coreholes at the Idaho National Engineering and Environmental Laboratory, Idaho*, M. S. Thesis: Idaho State University, Pocatello, Idaho.

Blair, J. J., and P. K. Link, 2000, "Pliocene and Quaternary Sedimentation and Stratigraphy of the Big Lost Trough from Coreholes at the Idaho National Engineering and Environmental Laboratory, Idaho: Evidence for a Regional Pliocene Lake during the Olduvai Normal Polarity Subchron," Robinson, L., ed., *Proceedings of the 35th Symposium on Engineering Geology and Geotechnical Engineering, Pocatello, Idaho, Idaho State University*.

Champion, D. E., M. A. Lanphere, and M. A. Kuntz, 1988, "Evidence for a New Geomagnetic Reversal from Lava Flows in Idaho—Discussion of Short Polarity Reversals in the Brunhes and Late Matuyama Polarity Chrons," *Journal of Geophysical Research*, Vol. 93, No. B10, pp. 11,677–11,680.

Champion, D. E., M. A. Lanphere, S. R. Anderson, and M. A. Kuntz, 2002, "Accumulation and subsidence of Late Pleistocene basaltic lava flows of the eastern Snake River Plain, Idaho," Link, P. K., and L. L. Mink, eds., *Geology, Hydrogeology, and Environmental Remediation, Idaho National Engineering and Environmental Laboratory, Eastern Snake River Plain*, Geological Society of America Special Paper 353, pp. 175–192.

Chase, G. H., W. E. Teasdale, D. A. Ralston, and R. G. Jenson, 1964, *Completion Report for Observation Wells 1 through 49, 51, 54, 55, 56, 80, and 81 at the National Reactor Testing Station, Idaho,* IDO-22045, U.S. Geological Survey, U.S. Atomic Energy Commission Idaho Operations Office, May 1964.

Graf, W. H., 1971, *Hydraulics of Sediment Transport*, New York: McGraw-Hill Book Co, 515 pp.

Helm-Clark, C. M., and D. W. Rodgers, 2004, "New $^{40}Ar/^{39}Ar$ Data from Pleistocene Basalts on the East Snake River Plain, Idaho, and Their Implications for the Subsurface Structure of the Big Lost Trough," *Rocky Mountain/Cordillera Joint Section Meeting of the Geological Society of America, Boise, Idaho, May 3–5, 2004,* Paper No. 46-1.

Helm-Clark, C. M., D. W. Rodgers, and R. P. Smith, 2004, "Borehole geophysical techniques to define stratigraphy, alteration, and aquifers in basalt," *Journal of Applied Geophysics*, Vol. 55, No. 1, pp. 3–38.

Hughes, S. S., M. McCurry, and D. J. Geist, 2002, "Geochemical correlations and implications for the magmatic evolution of basalt flow groups at the Idaho National Engineering and Environmental Laboratory," Link, P. K., and L. L. Mink, (eds.), *Geology, Hydrogeology, and Environmental Remediation, Idaho National Engineering and Environmental Laboratory, Eastern Snake River Plain*, Geological Society of America Special Paper 353, pp. 151–173.

Humphreys, E. D., K. G. Dueker, D. L. Schutt, and R. B. Smith, 2000, "Beneath Yellowstone: Evaluating plume and nonplume models using telesiesmic images of the upper mantle," *GSA Today*, Vol. 10, No. 12, pp. 1–7.

INEEL, 2003, *End of Well Report for Middle-1823 Waste Area Group 10 Deep Corehole Vertical Profile,* INEEL/EXT-03-00392, Revision 1, Idaho National Engineering and Environmental Laboratory, July 2003.

Jones, J. R., S. L. Jones, and E. G. Crosthwaite, 1953, *Logs of Test Holes in the Central Snake River Plain, Idaho,* IDO-22015, Supplement 1, p. 51.

Kuntz, M. A., H. R. Covington, and L. J. Schorr, 1992, "An overview of basaltic volcanism on the eastern Snake River Plain, Idaho," Link, P. K., M. A. Kuntz, and P. L. Platt, eds., *Regional Geology of Eastern Idaho and Western Wyoming,* Geological Society of America Memoir 179, pp. 227–267.

Kuntz, M. A., G. B. Dalrymple, D. E. Champion, and D. J. Doherty, 1980, *An Evaluation of Potential Volcanic Hazards at the Radioactive Waste Management Complex, Idaho National Engineering Laboratory, Idaho,* U.S. Geological Survey Open File Report 90-388, p. 68.

Kuntz, M. A., P. L. Link, D. L. Boyack, J. K. Geslin, L. E. Mark, M. K. V. Hodges, M. E. Kauffman, D. E., Champion, M. R. Lanphere, D. W. Rodgers, and M. H. Anders, 2003, "Geologic Map of the Northern and Central Parts of the Idaho National Engineering and Environmental Laboratory, Eastern Idaho," Idaho Geological Survey, Geologic Map 35.

Kuntz, M. A., B. Skipp, M. A. Lanphere, W. B. Scott, K. L. Pierce, G. B. Dalrymple, D. E. Champion, G. F. Embree, W. R. Page, L. A. Morgan, R. P. Smith, W. R. Hackett, and D. W. Rodgers, 1994, "Geological map of the Idaho National Engineering Laboratory and adjoining areas, eastern Idaho," United States Geological Survey Miscellaneous Investigations Series Map I-2330, scale 1:100,000.

Lanphere, M. A, D. E. Champion, and M. A. Kuntz, 1993, *Petrography, Age, and Paleomagnetism in Coreholes Well 80, NRF 89-04, NRF 89-05, and ICPP-123, Idaho National Engineering Laboratory,"* U.S. Geological Survey Open-File Report 93-327, p. 40.

LaPoint, P. J. L., 1977, "Preliminary Photogeologic Map of the Eastern Snake River Plain, Idaho," Map MF-850, U.S. Geological Survey Miscellaneous Field Studies.

Morse, L. H., and M. McCurry, 2002, "Genesis of alteration of Quaternary basalts within a portion of the eastern Snake River Plain aquifer," Link, P. K., and L. L. Mink, eds., *Geology, Hydrogeology, and Environmental Remediation, Idaho National Engineering and Environmental Laboratory, Eastern Snake River Plain, Idaho,* Geological Society of America Special Paper 353, pp. 213–224.

Paillet, F. L., and D. Boyce, 1996, *Analysis of Well Logs for Borehole ANL-OBS-A-001 at the Idaho National Engineering Laboratory, Idaho*, U.S. Geological Survey Open-File Report 96-213, p. 23.

Pierce, K. L., and L. A. Morgan, 1992, "The track of the Yellowstone hot spot: Volcanism, faulting, and uplift," Link, P. K., M. A. Kuntz, and L. B. Platt, eds., *Regional Geology of Eastern Idaho and Western Wyoming*, Geological Society of America Memoir 179, pp.1–53.

Reed, M. F., R. C. Bartholomay, and S. S. Hughes, 1997, "Geochemistry and stratigraphic correlation of basalt lavas beneath the Idaho Chemical Processing Plant, Idaho National Engineering Laboratory," *Environmental Geology*, Vol. 30 (1/2), pp. 108–118.

Rollinson, H., 1993, "Using Geochemical Data: Evaluation, Presentation, Interpretation," *Longman Scientific & Technical*, United Kingdom: Harlow.

Scarberry, K. C., 2003, *Volcanology, Geochemistry, and Stratigraphy of the F Basalt Flow Group, Eastern Snake River Plain, Idaho*, M. S. Thesis: Idaho State University, Pocatello, Idaho.

Smith, R. P., 2002, *Variability of the Aquifer Thickness Beneath the Idaho National Engineering and Environmental Laboratory*, INEEL/EXT-02-01022, Revision 0, Idaho National Engineering and Environmental Laboratory.

Wetmore, P.L., 1998, *An assessment of physical volcanology tectonics of the central eastern Snake River Plain based on correlation of subsurface basalts at and near the Idaho National Engineering and Environmental Laboratory, Idaho*, Master's Thesis: Idaho State University, Pocatello, Idaho, pp. 118.